# The *Mycobacterium bovis* Bacille Calmette-Guérin Phagosome Proteome*[S]

**Bai-Yu Lee‡, Deepa Jethwaney§¶, Birgit Schilling§, Daniel L. Clemens‡‖, Bradford W. Gibson§**, and Marcus A. Horwitz‡**

***Mycobacterium tuberculosis* and *Mycobacterium bovis* bacille Calmette-Guérin (BCG) alter the maturation of their phagosomes and reside within a compartment that resists acidification and fusion with lysosomes. To define the molecular composition of this compartment, we developed a novel method for obtaining highly purified phagosomes from BCG-infected human macrophages and analyzed the phagosomes by Western immunoblotting and mass spectrometry-based proteomics. Our purification procedure revealed that BCG grown on artificial medium becomes less dense after growth in macrophages. By Western immunoblotting, LAMP-2, Niemann-Pick protein C1, and syntaxin 3 were readily detectable on the BCG phagosome but at levels that were lower than on the latex bead phagosome; flotillin-1 and the vacuolar ATPase were barely detectable on the BCG phagosome but highly enriched on the latex bead phagosome. Immunofluorescence studies confirmed the scarcity of flotillin on BCG phagosomes and demonstrated an inverse correlation between bacterial metabolic activity and flotillin on *M. tuberculosis* phagosomes. By mass spectrometry, 447 human host proteins were identified on BCG phagosomes, and a partially overlapping set of 289 human proteins on latex bead phagosomes was identified. Interestingly, the majority of the proteins identified consistently on BCG phagosome preparations were also identified on latex bead phagosomes, indicating a high degree of overlap in protein composition of these two compartments. It is likely that many differences in protein composition are quantitative rather than qualitative in nature. Despite the remarkable overlap in protein composition, we consistently identified a number of proteins on the BCG phagosomes that were not identified in any of our latex bead phagosome preparations, including proteins involved in membrane trafficking and signal transduction, such as Ras GTPase-activating-like protein IQGAP1, and proteins of unknown function, such as FAM3C. Our phagosome purification procedure and initial proteomics analyses set the stage for a quantitative comparative analysis of mycobacterial and latex bead phagosome proteomes.** ***Molecular & Cellular Proteomics 9:32–53, 2010.***

*Mycobacterium tuberculosis*, the etiological agent of tuberculosis, is a facultative intracellular bacterium. In human macrophages, *M. tuberculosis* resides in a membrane-bound phagosomal compartment that resists fusion with lysosomes and is only mildly acidified (1–5). In previous studies, using the cryosection immunogold technique, we have found that the *M. tuberculosis* phagosome exhibits delayed clearance of major histocompatability complex class I molecules and relatively weak staining for lysosomal membrane glycoproteins CD63, LAMP-1,[1] and LAMP-2 and the lysosomal acid protease cathepsin D (6–10). Studies by other investigators have also demonstrated that *M. tuberculosis* and other mycobacterial species, including *Mycobacterium bovis* BCG, reside in phagosomes that resist acidification, are less mature, and less fusogenic with lysosomes than phagosomes containing inert particles (11–13). These results are consistent with the hypothesis that *M. tuberculosis* and *M. bovis* BCG retard the maturation of their phagosomes along the endolysosomal pathway and reside in a compartment that has not matured fully to a phagolysosome (7). Although the phagosomes of latex beads have been subjected to detailed proteomics analysis by Desjardins and co-workers (14), a detailed proteomics study of the *M. bovis* BCG phagosome has not been reported previously.

From the ‡Division of Infectious Diseases, Department of Medicine, Center for Health Sciences, University of California-Los Angeles School of Medicine, Los Angeles, California 90095-1688, §Buck Institute for Age Research, Novato, California 94945, and **Department of Pharmaceutical Chemistry, University of California, San Francisco, California 94143

Received, August 25, 2009

Published, MCP Papers in Press, October 7, 2009, DOI 10.1074/mcp.M900396-MCP200

[1] The abbreviations used are: LAMP, lysosome-associated membrane glycoprotein; Alix, programmed cell death 6-interacting protein; Arf, ADP-ribosylation factor; Arl, ADP-ribosylation factor-like; BASP1, brain acid-soluble protein 1; BCG, bacille Calmette-Guérin; BiP, Binding Protein; CAP1, adenylyl cyclase-associated protein 1; CHMP4b, charged multivesicular body protein 4b; ER, endoplasmic reticulum; GFP, green fluorescent protein; GNAI2, guanine nucleotide-binding protein $G_i$, $\alpha$-2 subunit; HB, homogenization buffer; HRP, horseradish peroxidase; IPTG, isopropyl $\beta$-D-1-thiogalactopyranoside; LAM, lipoarabinomannan; M6PR, mannose 6-phosphate receptor; *Mtb*-iGFP, *M. tuberculosis* with inducible GFP expression; MVB, multivesicular body; NPC1, Niemann-Pick protein C1; PMA, phorbol 12-myristate 13-acetate; PNS, postnuclear supernate; RPMI, Roswell Park Memorial Institute; SPFH, stomatin, prohibitin, flotillin, HflK/C; ATPase, vacuolar ATPase; VAT-1, vesicle amine transport membrane protein-1; VDAC, voltage-dependent anion channel; HI-FBS, heat-inactivated fetal bovine serum; GDI, guanine dissociation inhibitor.

We describe in this study a novel method for the purification of the BCG phagosome from infected human macrophages, a detailed proteomics analysis of the BCG phagosome, and a comparison of the phagosome with latex bead phagosomes isolated from human macrophages. This study is the first comprehensive proteomics study of the *M. bovis* BCG phagosome and the first mass spectrometry-based proteomics study of the latex bead phagosome in human macrophages. We showed by Western immunoblotting that, relative to latex bead phagosomes, the BCG phagosome is relatively depleted in LAMP-2, NPC1, flotillin-1, vATPase, and syntaxin 3. Remarkably, by mass spectrometry, we documented a high degree of overlap in the set of proteins on BCG and latex bead phagosomes but also noteworthy differences. Novel proteins detected on the BCG phagosome but not on the latex bead phagosome include CD44, intercellular adhesion molecule 1, protein FAM3C, Ral-A/Ral-B, stress-induced phosphoprotein 1, band 4.1-like protein 3, septin-7, Ras GTPase-activating protein-like protein IQGAP1, Rab-6A, erlin-2, and tumor protein D54. Conversely, proteins identified on latex bead phagosomes but not on the BCG phagosome are $\beta$-galactosidase and sialate *O*-acetylesterase.

## EXPERIMENTAL PROCEDURES

*Primary and Secondary Antibodies*—Monoclonal and polyclonal antibodies were purchased from the following sources: goat anti-rabbit IgG horseradish peroxidase (HRP) conjugate and rabbit anti-goat IgG HRP conjugate from Bio-Rad; chicken antibody to vATPase subunit 6E and goat anti-chicken IgY-Fc HRP conjugate from Gen-Way; rabbit antibody to stathmin and goat anti-mouse IgG HRP conjugate from Sigma; rabbit monoclonal antibody to flotillin-1, rabbit polyclonal antibodies to the 60-kDa mitochondrial antigen, clathrin, and Rab-11, and mouse monoclonal antibody to calnexin from Abcam; mouse monoclonal antibodies to Ral-B and syntaxin 3 and rabbit polyclonal antibody to Niemann-Pick protein C1 from Abnova; mouse monoclonal antibody to voltage-dependent anion channel (VDAC)-1 from MitoSciences; goat anti-galectin-1 antibody from R&D Systems, Inc.; mouse monoclonal antibody to Binding Protein (BiP) from BD Transduction Laboratories; mouse monoclonal antibody to calreticulin and rabbit antibody to manganese superoxide dismutase from Stressgen; mouse monoclonal antibody to LAMP-2 from the University of Iowa Hybridoma Bank (Iowa City, Iowa); and mouse monoclonal antibody to cathepsin D from Santa Cruz Biotechnology, Inc. Mouse monoclonal antibody to lipoarabinomannan (LAM) (clone CS35) was generously provided by Dr. John Belisle, Colorado State University, Fort Collins, CO. Rabbit antibody to *M. tuberculosis* LAM was prepared as described previously (15).

*Bacterial Strains and Growth Conditions*—Bacterial strains were stored at −80 °C in Middlebrook 7H9 medium with 10% oleic acid, albumin, dextrose, catalase enrichment additive for Middlebrook medium enrichment and 20% glycerol. Recombinant *M. tuberculosis* Erdman strain (ATCC 35801) expressing $GFP_{UV}$, *M. tuberculosis* expressing an IPTG-inducible $GFP_{UV}$, and recombinant *M. bovis* BCG expressing $GFP_{UV}$ were prepared as described previously (15, 16); grown on Middlebrook 7H11 agar at 37 °C in 5% $CO_2$, 95% air atmosphere; and scraped from agar plates immediately prior to use in infection experiments. Prior to use of bacteria for infection of human macrophages, bacterial aggregates were dispersed by sonication of the bacteria in a water bath sonicator (Astrason Scientific) for eight periods of 15 s with cooling of the suspension in an ice bath for 5 s between sonications. Residual aggregates were removed by centrifugation at 200 × *g* for 10 min at 4 °C. The pellet of aggregated bacteria was discarded, the supernatant suspension was centrifuged again under the same conditions, and the process was repeated a total of three times. Phase and fluorescence microscopy of the final supernatant confirmed that the suspension consisted almost entirely of single bacteria.

*Preparation of Formalin-killed GFP-M. tuberculosis*—GFP-expressing *M. tuberculosis* prepared as described previously (15) were plated on 7H11 agar plates containing hygromycin; incubated at 37 °C in 5% $CO_2$, 95% air for 10–14 days; and scraped into Dulbecco's PBS (Irvine Scientific Co.), and aggregates were removed by water bath sonication and low speed centrifugation as described above. Paraformaldehyde was added to the bacterial suspension to a final concentration of 4% paraformaldehyde. After 30 min at room temperature, the formalin-killed bacteria were washed three times in PBS by centrifugation at 10,000 × *g* for 10 min. Because washing by centrifugation induces aggregation, bacterial aggregates were removed by centrifugation at 200 × *g* for 10 min immediately prior to use of the formalin-killed bacteria in an infection experiment.

*THP-1 Cells*—The human monocytic cell line THP-1 (ATCC, TIB-202) was grown in RPMI 1640 medium (Mediatech, Herndon, VA) supplemented with 2 mM glutamine, 10% heat-inactivated fetal bovine serum (HI-FBS), 1000 IU/ml penicillin, and 100 $\mu$g/ml streptomycin. Prior to use in an infection experiment, the THP-1 cells were added to glass coverslips in 2-$cm^2$ tissue culture wells ($2 \times 10^5$ cells/$cm^2$) or to 225-$cm^2$ tissue culture flasks (30 million cells per flask) and differentiated with phorbol 12-myristate 13-acetate (PMA; 100 nM) in RPMI 1640 medium with 10% HI-FBS for 3 days at 37 °C in air containing 5% $CO_2$.

*Purification of 3-h BCG and Latex Bead Phagosomes*—BCG-GFP were plated on 7H11 agar plates; cultured at 37 °C for 10 days in a 5% $CO_2$, 95% air environment; scraped into RPMI 1640 medium containing 20 mM HEPES, pH 7.4; sonicated in a water bath; and centrifuged to remove aggregates as described above. The bacteria were adjusted to an optical density (540 nm) of 0.1 in 10% human serum (blood type AB), and 15 ml of the bacterial suspension were added to monolayers of THP-1 cells in each of 12 225-$cm^2$ culture flasks (multiplicity of infection of 80:1, bacteria to macrophage). Green fluorescent latex beads (1-$\mu$m diameter, 2% solids; Polysciences) were diluted 1:500 in 10% human serum (type AB) in RPMI 1640 medium, and 15 ml of the bead suspension were added to monolayers of THP-1 cells in each of 12 225-$cm^2$ culture flasks. The cultures were incubated for 2 h at 37 °C, washed with RPMI 1640 medium to remove non-adherent bacteria or beads, incubated for an additional 1 h at 37 °C in RPMI 1640 medium containing 10% HI-FBS, and washed twice with PBS, and the monolayers were scraped into homogenization buffer (0.25 M sucrose, 0.5 mM EGTA, 20 mM HEPES, pH 7.4) containing protease inhibitors (Set III, Calbiochem; 1:1000 dilution) and 5 $\mu$g/ml cytochalasin. (Cytochalasin is added to decrease the clumping of organelles in a cytoskeletal meshwork.) The cell suspension was homogenized with a motor-driven Teflon/glass Dounce homogenizer, and the progress of cell disruption was followed by phase and fluorescence microscopy. Homogenization was stopped when at least 70% of the macrophages appear disrupted (8–12 strokes). Benzonase was added to the homogenate (25,000 units/ml), and the homogenate was incubated at 37 °C for 5 min to degrade DNA that can cause artifactual clumping of organelles. The homogenate was centrifuged at 200 × *g* for 10 min, the supernatant was removed and centrifuged again under the same conditions, and the process was repeated for a total of three centrifugations; the resulting supernatant was designated the postnuclear supernatant (PNS). The PNS was transferred to a 50-ml centrifuge tube and underlaid with a step gradient consisting of 5 ml each of 15% (w/w)

and 50% (w/v) sucrose. These and all sucrose and iodixanol solutions contained 0.5 mM EGTA and 20 mM HEPES, pH 7.4. The step gradients were centrifuged at 1000 × *g* for 45 min (BCG) or at 2000 × *g* for 1 h (latex beads), and fractions were collected from the bottom of the tubes. Bacterial phagosomes and bead phagosomes were collected from the 15–50% sucrose interface, and 50% (w/v) sucrose was added to the samples to yield a final concentration of 40% (w/v) sucrose. A step gradient consisting of 5 ml of 10, 25, and 35% (w/v) sucrose was prepared, and the step gradient was underlaid with the sample (40% sucrose, w/v). The sample was then underlaid sequentially with 55% sucrose, 65% sucrose, and 50% iodixanol (50% iodixanol is more dense than 65% sucrose). The gradient was centrifuged at 10,000 × *g* for 20 h, fractions were collected from the bottom of the tube, and fractions containing BCG-GFP and the fluorescent beads were identified by fluorescence microscopy. The BCG-GFP were found at the 40–55% sucrose interface, and the latex beads were found at the 10–25% sucrose interface. The latex beads from the 10–25% sucrose interface were diluted with 2 volumes of HB and pelleted by centrifugation at 2000 × *g* for 60 min. The BCG-GFP were mixed with 50% iodixanol to achieve a final concentration of 30% iodixanol, and the sample was underlaid beneath a 10–30% linear iodixanol gradient and centrifuged at 50,000 × *g* for 5 h. The gradient was fractionated from the bottom, and the location of GFP-BCG bacteria was determined by fluorescence microscopy to be at a region of the gradient corresponding to 18% iodixanol. The fractions containing the BCG-GFP were mixed with 1 volume of HB and pelleted by centrifugation at 1000 × *g* for 45 min.

*Purification of 1–5-day BCG and Latex Bead Phagosomes*—PMA-differentiated THP-1 cells were incubated overnight with either fluorescent green latex beads (1:500 suspension of 2% solids) or BCG-GFP at a multiplicity of infection of 80:1 as described above. Non-adherent latex beads or BCG-GFP were washed away, and the macrophages were incubated for an additional 3 h, 2 days, or 4 days at 37 °C in 5% $CO_2$ for the 1-, 3-, and 5-day time points, respectively. The macrophage monolayers were washed twice with PBS and once with HB, scraped into HB containing cytochalasin and protease inhibitors (1:1000 dilution), and homogenized with a Dounce homogenizer, and a PNS was obtained as described above. For purification of latex beads, the PNS was layered over a 25–50% (w/w) sucrose step gradient and centrifuged at 2000 × *g* for 45 min, and fractions were collected from the bottom. The latex bead phagosomes were collected at the PNS/25% sucrose interface, and 50% (w/w) sucrose was added to achieve a final concentration of 40% (w/w) sucrose. The sample was transferred to a centrifuge tube, underlaid sequentially with 55% sucrose and 50% iodixanol, and overlaid sequentially with 35, 25, and 10% sucrose. The step gradient was centrifuged at 100,000 × *g* for 2 h and fractionated from the bottom, and the location of the latex beads at the 10–25% sucrose interface was verified by phase and fluorescence microscopy. The fractions containing the latex beads were diluted with 2 volumes of HB and pelleted by centrifugation at 2000 × *g* for 45 min, and the pellet was resuspended in SDS-PAGE sample buffer for analysis by Western immunoblotting and mass spectrometry-based proteomics. For purification of BCG phagosomes, the PNS was transferred to a centrifuge tube and underlaid with 5 ml of 15% sucrose (w/w), which in turn was underlaid with 5 ml of 30% iodixanol. The step gradient was centrifuged at 1000 × *g* for 45 min and fractionated from the bottom, and the bacterial phagosomes were collected from the 15% sucrose/30% iodixanol interface. The sample was mixed with 50% iodixanol to achieve a final concentration of 30–35% iodixanol. A linear 25–10% iodixanol gradient was prepared in a new centrifuge tube and underlaid sequentially with the sample (30–35% iodixanol) and 1 ml of 50% iodixanol and centrifuged at 50,000 × *g* for 4 h, and fractions were collected from the bottom of the gradient. The number of BCG-GFP per fraction was determined by phase and fluorescence microscopy. The peak fraction was mixed with 2 volumes of HB and layered over a sucrose step gradient of 25, 30, 35, 40, 50, 55, and 65% (w/v) sucrose and centrifuged at 10,000 × *g* for 12–14 h at 4 °C. The BCG phagosomes (with a density of 35% sucrose) were diluted 2-fold with HB and pelleted by centrifugation at 1000 × *g* for 45 min. The pellet was resuspended either in SDS-PAGE sample buffer for proteomics analysis and Western immunoblotting or mixed with 2.5% glutaraldehyde and 1% osmium tetroxide in 0.1 M sodium cacodylate, pH 7.3; embedded in agarose; poststained with 2% uranyl acetate in 0.1 M sodium acetate, pH 6.3; dehydrated through a graded series of ethanol; infiltrated and embedded in Epon 828 epoxy resin; and processed for transmission electron microscopy as described previously (17).

To obtain a quantitative assessment of purity of our 3-day BCG phagosomes, we used the radioisotopic mixing method described by Chakraborty *et al.* (18). Briefly, flasks of PMA-differentiated THP-1 cells were either left uninfected or were infected as described above. Twelve hours prior to harvest, uninfected flasks and infected flasks were either metabolically radiolabeled by addition of [$^{35}$S]cysteine/methionine (PerkinElmer Life Sciences; 0.25 mCi in cysteine/methionine-free RPMI 1640 medium containing 10% HI-FBS) or not radiolabeled. To determine the number of "false phagosome counts," we added a flask of radiolabeled, uninfected macrophages to non-radiolabeled, infected macrophages. To determine the number of "true phagosome counts," we added a radiolabeled, infected flask with the same amount of radioactivity to the same number of uninfected macrophages as used in the "false phagosome count" preparation. The phagosome purification protocol was followed identically for the "true" and "false" phagosome count preparations. The degree of purification was calculated as $(T - F)/T$ where "*T*" represents true phagosome counts and "*F*" represents false phagosome counts.

*Western Immunoblotting*—The proteins in the bacterial or latex bead phagosome samples were separated by SDS-PAGE and electrophoretically transferred onto a nitrocellulose membrane. The membrane was incubated with mouse, rabbit, goat, or chicken primary antibody to the antigen of interest, washed, incubated with the appropriate HRP-conjugated secondary antibody, washed, and developed with SuperSignal West Pico chemiluminescent substrate (Pierce), and the signal from immunoreactive protein bands was detected by exposing the membrane to x-ray film.

*Immunofluorescence Staining of Flotillin-1 in THP-1 Cells*—Monolayers of differentiated THP-1 cells on coverslips were co-incubated for 90 min with fluorescent blue latex beads (Polysciences; 1-$\mu$m diameter, at a 4000-fold dilution of a stock suspension of 10% solids), BCG-GFP, *M. tuberculosis*-iGFP, or formalin-killed GFP-*M. tuberculosis* suspended in RPMI 1640 medium containing 10% fresh AB serum. Monolayers were washed with culture medium; incubated in fresh medium with or without 1 mM IPTG at 37 °C for 48–72 h; fixed in 4% paraformaldehyde in 0.075 M sodium phosphate buffer, pH 7.4 for 30 min at room temperature; permeabilized in 0.1% saponin in PBS containing 10 mM glycine; and incubated with 5% goat serum in PBS with 1% BSA to block nonspecific staining. Coverslips were stained with rabbit monoclonal antibody to human flotillin-1 (1:50 dilution in the same buffer) overnight at 4 °C. Coverslips were washed with PBS and incubated with Texas Red-conjugated goat anti-rabbit IgG (diluted 1:50 in the same buffer) for 90 min at room temperature. The coverslips were washed in PBS, incubated with mouse monoclonal antibody to LAM (5 $\mu$g/ml; CS35), washed in PBS, stained with coumarin-conjugated goat-anti-mouse IgG (Sigma; 1:50 dilution), post-fixed in 2% paraformaldehyde in PBS, incubated with 2.5 $\mu$M 4′-6-diamidino-2-phenylindole in PBS for 15 min at room temperature to label host nuclei, washed in PBS, blotted, mounted with Prolong Antifade mounting medium (Molecular Probes), and viewed by epif-

luorescence microscopy with an Eclipse TE2000-S microscope equipped with an X-Cite 120 light source (Nikon), and images were acquired with a SPOT RT-KE monochrome camera and SPOT software (Diagnostic Instruments, Sterling Heights, MI) and by confocal scanning microscopy with a Leica TCS-SP confocal and two-photon microscope and Leica confocal software. Texas Red, Oregon Green, and 4′-6-diamidino-2-phenylindole fluorochromes were excited with confocal krypton and argon lasers and two-photon scanning with a short pulsed titanium-sapphire laser, respectively. Confocal microscopy was performed in the Carol Moss Spivak Cell Imaging Facility at the University of California at Los Angeles Brain Research Institute.

*In-gel Tryptic Digestion of Proteins*—The final pellets of phagosome preparations were resuspended in SDS-PAGE sample buffer, boiled for 5 min, electrophoresed on precast polyacrylamide 8–16% gradient gels (Bio-Rad), and stained by SYPRO Ruby protein stain (Invitrogen) according to the manufacturer's directions. The protein bands visualized by SYPRO Ruby staining were labeled from top to bottom in each lane, excised using a 1.5-mm gel picker (P2D1.5, The Gel Co., San Francisco, CA), and processed with an automatic in-gel digester robot, ProGest (Genomic Solutions, Ann Arbor, MI). Processing steps consisted of destaining and dehydrating the excised gel slices with acetonitrile, reduction with 10 mM DTT at 60 °C for 30 min, alkylation of cysteine residues with 100 mM iodoacetamide (37 °C for 45 min), and proteolytic digestion using 125–250 ng of sequencing grade trypsin (Promega, Madison, WI) at 37 °C for 4 h. The resulting tryptic peptides were then extracted from the gel by aqueous/10% formic acid extraction and analyzed by mass spectrometry (19).

*Mass Spectrometry*—The proteolytic peptide mixtures obtained from digested gel spots were analyzed by reverse-phase nano-HPLC-ESI-MS/MS. Briefly, peptides were separated on an Ultimate nanocapillary HPLC system equipped with a Magic C18AQ nanocolumn (75-$\mu$m inner diameter $\times$ 15 cm) and CapTrap Micro guard column of 0.5-$\mu$l bed volume (both Michrom Bioresources, Inc., Auburn, CA). Peptide mixtures were loaded onto the guard column and washed with the loading solvent (0.05% formic acid; flow rate, 20 $\mu$l/min) for 5 min, then transferred onto the analytical $C_{18}$ nanocapillary HPLC column, and eluted at a flow rate of 300 nl/min using the following gradient: 2% solvent B in A (from 0 to 5 min) and 2–70% solvent B in A (from 5 to 55 min). Solvent A consisted of 0.05% formic acid in 98% $H_2O$, 2% ACN, and solvent B consisted of 0.05% formic acid in 98% ACN, 2% $H_2O$. The column eluant was directly coupled to a "QSTAR Pulsar i" quadrupole orthogonal TOF mass spectrometer (MDS Sciex) equipped with a Protana nanospray ion source (Proxeon Biosystems). The nanospray needle voltage was typically 2300 V in the HPLC-MS mode. Mass spectra (ESI-MS) and tandem mass spectra (ESI-MS/MS) were recorded in positive ion mode with a resolution of 12,000–15,000 full-width half-maximum. For CID-MS/MS, the mass window for precursor ion selection of the quadrupole mass analyzer was set to $\pm$1 *m/z*. The precursor ions were fragmented in a collision cell using nitrogen as the collision gas. Spectra were calibrated in static nanospray mode using MS/MS fragment ions of a renin peptide standard (His immonium ion with *m/z* at 110.0713 and $b_8$-ion with *m/z* at 1028.5312). Because a 1D SDS-PAGE separation approach excising contiguous gel bands with up to 50 gel slices per gel lane (and per biological experiment) was used, subsequently after in-gel digestion, long QSTAR pulsar HPLC run sequences were set up to account for all samples (typically a non-interrupted MS run time of 2–3 days).

*Database Searches*—Mass spectrometric data were analyzed with an in-house licensed bioinformatics database search engine system, Mascot version 2.2.04 (Matrix Sciences, London, UK) (20). Peak lists for the QSTAR pulsar i LC-MS/MS data sets were generated using the Mascot.dll script version 1.6b19 for Analyst QS 1.0 (parameters used were: remove peaks with intensity less than 0.1% of the highest peak; centroid all MS/MS data; merge distance, 0.02). Files were submitted to the Mascot search engine using Mascot Daemon version 2.2.2. Mascot uses a probability-based "Mowse score" to evaluate data obtained from tandem mass spectra. The following search parameters were used: enzyme specificity was defined as trypsin; carbamidomethyl (Cys) was chosen as fixed modification; acetyl (protein N-terminal), Gln $\rightarrow$ pyro-Glu (N-terminal Gln), and oxidation (Met) were chosen as variable modifications; mass tolerance for precursor ions was 250 ppm; and mass tolerance for fragment ions was 0.4 Da. The publicly available Swiss-Prot database release version 56.2 (release September 23, 2008) was searched for most data obtained from human samples with species restriction "human" (20,407 sequences); some data obtained from mouse samples were searched with species restriction "*Mus musculus*" (15,931 sequences). Ions scores are $[-10 \times \log(p)]$ where $p$ is the probability that the observed match is a random event. For human Mascot database searches, a cutoff expectation value of 0.05 (significance threshold) was chosen for individual MS/MS spectra that resulted in a false discovery rate of 2.9% (automatic decoy database search). All data sets were also searched using the Mascot search engine against a custom database representing the complete proteome of *M. bovis* strain BCG/Pasteur 1173P2 (21). The number of protein entries with species code MYCBP within the UniProt Knowledgebase was 3891. Very high false discovery rates were calculated that consequently did not allow confident *M. bovis* protein identification. In addition, we searched the *M. bovis*_BCG_Pasteur_1173P2 database (total proteins used, 3952) using the Global Proteome Machine search engine. However, the Global Proteome Machine engine reported only random matches. For mouse Mascot database searches, a cutoff expectation value of 0.02 (significance threshold) was chosen for individual MS/MS spectra that resulted in a false discovery rate of 2.1% (automatic decoy database search). For LC-MS/MS acquired data, a minimum of two observed significant peptides that were selected for tandem mass spectrometry was required to confirm protein identification. In the few cases where only one unique peptide per protein was selected for MS/MS, the MS/MS spectrum was inspected "manually" based on an adaptation of previously published criteria (22), and the protein was thus confirmed or deleted from the identification list. Specifically, proteins with only one observed peptide were validated and added to the list only if the following criteria were satisfied. 1) The peptide represented a unique peptide in the human proteome as confirmed by BLAST searches. (2) Manual inspection of the spectrum verified the following criteria: (*a*) good signal to noise (signal to noise ratio $>$3 for the majority of fragment ions), (*b*) a minimum of three consecutive y- or b-ions, (*c*) any y-ion with an N-terminal proline must be intense, and (*d*) an immonium ion for Arg (*m/z* 175.12) or Lys (*m/z* 147.11) must be present that is consistent with the expected C-terminal tryptic site. As an additional criterion, we required that each specific protein assignment based on a single peptide identification was observed in more than one independent biological experiment either as part of a regular protein assignment observed together with multiple other peptides for that specific protein or as another single peptide-based protein assignment.

## RESULTS

### *Purification of BCG Phagosomes and Latex Bead Phagosomes*

We initially attempted to purify BCG phagosomes using density gradient techniques described previously for bacterial phagosomes (11, 23). However, we observed that the buoyant density of BCG and of *M. tuberculosis* depends on the culture conditions and that bacteria initially grown on agar or in liquid medium become lighter after growth in macro-

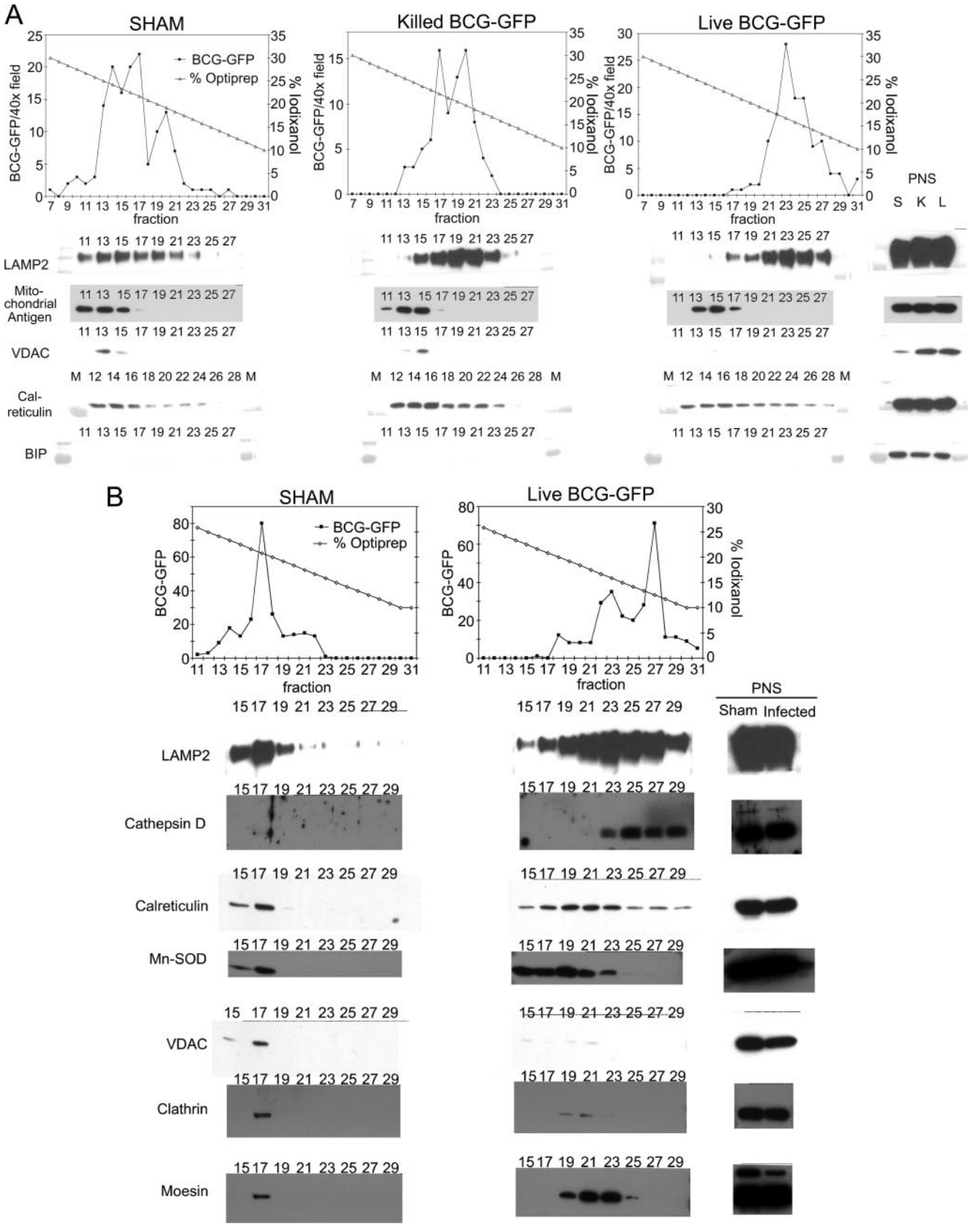
A
SHAM
Killed BCG-GFP
Live BCG-GFP
BCG-GFP
% Optiprep
BCG-GFP/40x field
% Iodixanol
fraction
PNS
S K L
LAMP2
Mito-chondrial Antigen
VDAC
Cal-reticulin
BIP
B
SHAM
Live BCG-GFP
BCG-GFP
% Iodixanol
fraction
PNS
Sham Infected
LAMP2
Cathepsin D
Calreticulin
Mn-SOD
VDAC
Clathrin
Moesin

phages. Whereas *M. tuberculosis* and BCG grown on 7H11 agar plates or in detergent-free 7H9 broth sedimented into 55% (w/v) sucrose, *M. tuberculosis* and BCG grown for 1 or more days within macrophages became much lighter and sedimented in the range of 31–35% sucrose. Therefore, purification strategies that rely on sedimentation of bacterial phagosomes through 55% sucrose as described previously for intracellular parasite phagosomes (11, 23) were not applicable to BCG or *M. tuberculosis* obtained from human macrophage culture. The buoyant density of BCG, assessed in iso-osmotic iodixanol density gradients, was also dramatically decreased after growth in macrophages. Whereas BCG freshly scraped from 7H11 agar plates exhibited a density of 1.114 on iodixanol gradients (corresponding to 20% iodixanol; Fig. 1, "sham" BCG phagosome gradients), BCG harvested after 3 days of growth in human THP-1 macrophages exhibited a much lighter density of 1.091 (corresponding to 12% iodixanol; Fig. 1, "live BCG-GFP"). Similarly, *M. tuberculosis* freshly harvested from agar plates exhibited a density of 1.126 in iodixanol gradients, whereas bacteria harvested after 1 day of growth in macrophage monolayers exhibited a density of 1.106 on iodixanol gradients. Killed BCG phagosomes exhibited a density similar to that of bacteria freshly harvested from plates (Fig. 1). This phenomenon is not attributable to selective uptake of less dense bacteria by macrophages because, in a separate experiment in which THP-1 macrophage monolayers were infected with agar plate-grown BCG that had been pelleted through 19% iodixanol (to remove less dense bacteria), the BCG harvested from the macrophages after 3 days of growth exhibited a density of 1.094 (corresponding to 13% iodixanol).

Because BCG became lighter with growth in macrophages, we purified BCG phagosomes from mouse J774 macrophages and from human THP-1 macrophages by using a combination of differential centrifugation and flotation on iodixanol density gradients. After obtaining a PNS, we removed the majority of contaminating organelles by low speed centrifugation (1000 $\times$ *g* for 45 min) through 15% sucrose onto a cushion of 30% iodixanol. Whereas mycobacterial phagosomes sediment through the 15% sucrose under these conditions, the majority of macrophage organelles and cytosolic constituents do not (13, 18). A substantial portion of the remaining contaminating organelles are removed by flotation of the phagosomes on an iodixanol density gradient, a technique that exploits the relatively unique low density of the mycobacteria in this iso-osmotic density gradient medium. Additional purification is obtained by sucrose density gradient sedimentation and the final low speed sedimentation, which pellets the bacterial phagosomes. In comparisons of true BCG phagosome and sham phagosome preparations run simultaneously under the same conditions, we observed relatively little contaminating protein in the sham phagosome preparations prepared from the density gradient fractions corresponding to those of the true BCG phagosome preparations (prepared from infected macrophages) (Fig. 2). We found that this technique also works well with mouse J774 macrophages, yielding a BCG phagosome preparation with more than 10-fold the protein content of that found in the corresponding sham phagosome preparation (supplemental Fig. 1).

Proteins present in the SDS-PAGE gels of purified BCG phagosomes are almost exclusively host macrophage (human) proteins. We found that *M. tuberculosis* and BCG proteins are not extracted under the conditions that we use to extract host phagosomal proteins (heating at 100 °C for 5 min in SDS-PAGE sample buffer), and thus mycobacterial proteins do not contribute significantly to the protein staining seen in our SDS-PAGE gels of phagosomal preparations. This is

FIG. 1. **Sedimentation of *M. bovis* BCG phagosomes from THP-1 cells on iodixanol density gradients 3 days postinfection.** *A*, human THP-1 macrophages were allowed to phagocytose live or killed *M. bovis* BCG-GFP or left untreated (*SHAM*), and a phagosomal fraction was purified 3 days postinfection. The sham phagosome preparations were processed identically to the other phagosome preparations except that *M. bovis* BCG was added to the macrophages at the end rather than the start of the incubation period and immediately prior to homogenization. Macrophages from all preparations were homogenized, PNS fractions were obtained by low speed centrifugation, and a phagosomal fraction was obtained by centrifugation through 15% sucrose onto 30% iodixanol. The BCG phagosomes (and free BCG in the case of the sham preparation) were collected from the interface and applied to linear iodixanol gradients. Gradient fractions were collected from the bottom, and aliquots representing equal fractions of the iodixanol gradient or the PNS (0.06% of the entire gradient or 0.06% of the total PNS, respectively) were analyzed by one-dimensional SDS-PAGE and Western immunoblotting. The relative number of BCG-GFP per gradient fraction was determined by mixing equal aliquots of each fraction with formaldehyde and counting the number of green fluorescent bacteria per 400$\times$ field by fluorescence microscopy. The BCG phagosomes are lighter than the majority of the mitochondria and ER and go to higher numbered fractions. Whereas LAMP-2 co-sediments with the BCG phagosomes, the mitochondrial antigen markers and the ER markers (calreticulin and BiP) are predominantly found in denser fractions. Whereas the mitochondrial marker VDAC and the ER marker BiP are abundant in the PNS, the majority of these organelles were removed in the purification step prior to the linear iodixanol gradient (low speed sedimentation through 15% sucrose) and thus are present at low levels in the iodixanol gradient fractions. *S*, sham; *K*, killed BCG; *L*, live BCG; M, molecular mass marker lane. *B* shows an independent replication of the purification of live and sham BCG phagosomes on an iodixanol gradient with analysis of gradient fractions by SDS-PAGE and Western immunoblotting for organelle markers. The BCG phagosomes co-elute with strong bands of LAMP-2 and cathepsin D. As is the case in *A*, the majority of ER and mitochondria are removed at the step prior to the linear iodixanol gradient. Some residual ER is apparent by calreticulin staining, mostly in fractions that are denser (lower numbered fractions) than the BCG phagosomes, although some calreticulin does co-elute. The mitochondria (stained by the mitochondrial antigens manganese superoxide dismutase (*Mn-SOD*) and VDAC) also elute in fractions that are denser than the BCG phagosomes. Clathrin (present on plasma membrane) and moesin (a cytoskeletal marker) are abundant in the PNS but are not detected by immunostaining in the peak fractions containing the BCG phagosomes.

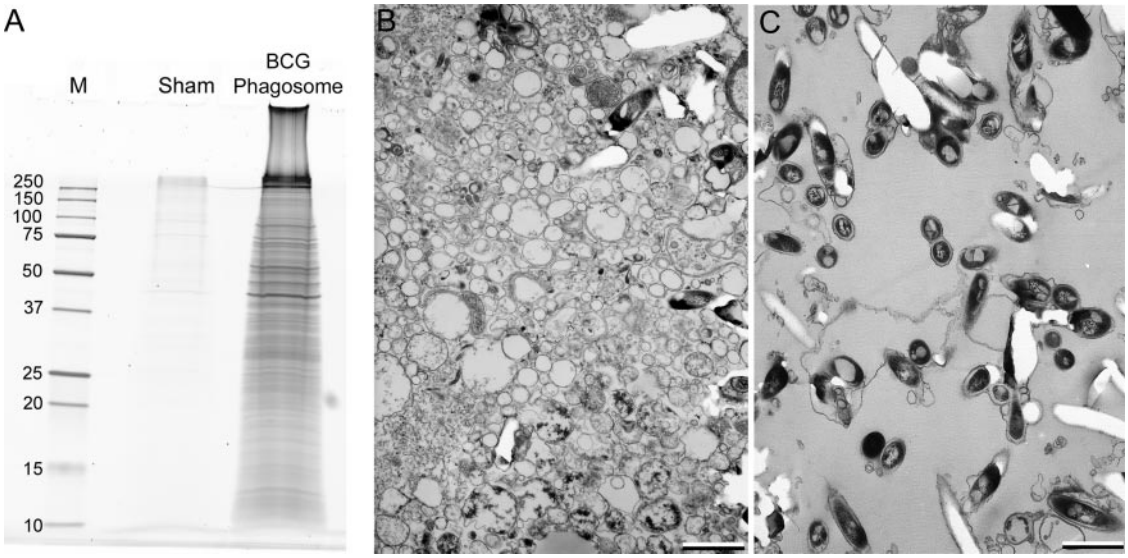


FIG. 2. **Analysis of BCG phagosomes purified 3 days postinfection from THP-1 cells by SDS-PAGE and electron microscopy.** *A*, BCG phagosomes purified from THP-1 cells 3 days after infection (*BCG Phagosome*) and sham phagosomes (*Sham*) prepared from identically treated, non-infected THP-1 cells to which BCG bacteria were added at the end rather than the beginning of the incubation period and immediately prior to homogenization were applied to a one-dimensional SDS-PAGE gradient gel and stained for protein by SYPRO Ruby. Masses of standard molecular mass markers (lane labeled "*M*") are indicated in kDa. *B* and *C*, transmission electron microscopy of the PNS starting material (pelleted by centrifugation at 10,000 × *g* for 10 min) (*B*) and the final purified BCG-GFP phagosomal pellet (*C*) demonstrates that the purified phagosomes (*C*) have relatively little contamination and are considerably enriched in BCG phagosomes compared with the PNS starting material (*B*). *Size bars*, 1 μm.

probably attributable to the detergent-resistant, thick, waxy cell wall present on the mycobacteria. Likewise, we did not identify any mycobacterial proteins in our mass spectrometry-based proteomics analysis, although mycobacterial LAM was abundant in the preparations, and mycobacteria appeared to constitute the majority of the biomass as seen by electron microscopy of the purified phagosomes (Fig. 2).

To assess the purity of our BCG phagosome preparations and to explore the presence or absence of selected antigenic proteins, we analyzed gradient fractions by Western immunoblotting. We observed that whereas the late endosomal-lysosomal marker LAMP-2 (Fig. 1, *A* and *B*) and the acid hydrolase cathepsin D (Fig. 1*B*) correspond well to the distribution of BCG-GFP from infected macrophages on the iodixanol gradient, the mitochondrial markers, VDAC (Fig. 1, *A* and *B*), the 60-kDa mitochondrial antigen (Fig. 1*A*), and manganese superoxide dismutase (Fig. 1*B*), were found in lower (more dense) fractions and were not detected by Western immunoblotting in the fractions containing the BCG phagosomes. Although the peak of the ER marker calreticulin was found in relatively dense fractions (Fig. 1*A*, fractions 12–16 of the live BCG-GFP gradient, and Fig. 1*B*, fractions 19–23 of the live BCG-GFP gradient), this marker consistently trailed into the lighter fractions containing the BCG-GFP phagosomes (Fig. 1*A*, peak fraction 23 of the live BCG-GFP gradient and Fig. 1*B*, peak fraction 27 of the live BCG-GFP gradient). We observed a similar trailing of calnexin into the 3-day BCG phagosome fractions (data not shown) and a similar profile for LAMP-2, mitochondrial VDAC, and calreticulin relative to BCG phagosomes on iodixanol gradients prepared from THP-1 macrophages at 3 h postinfection (supplemental Fig. 2). We also observed an association of calreticulin and other ER markers with latex bead phagosomes purified by sucrose density flotation (supplemental Fig. 2), consistent with prior reports regarding highly purified latex bead phagosomes from mouse J774 macrophages (14, 24). Whether the presence of calreticulin and calnexin in regions of the iodixanol gradient containing BCG phagosomes and latex bead phagosomes reflects a specific contribution of ER to the phagosome, as has been reported in the case of phagosomes containing latex beads, killed bacteria, zymosan, (14, 24–26), *Toxoplasma gondii* (27), and *M. tuberculosis* (28), or instead reflects contamination (29) remains to be determined. Clathrin, present on the plasma membrane and Golgi apparatus (30), was detected in the PNS but was absent from the gradient fractions containing the BCG phagosomes (Fig. 3*B*). Similarly, the cytoskeletal component moesin was stained intensely in the PNS but was relatively depleted in the gradient fractions corresponding to the BCG phagosomes (Fig. 1*B*).

We also examined the purity of our BCG phagosome preparations at the ultrastructural level by transmission electron microscopy (Fig. 2, *B* and *C*) and observed that the BCG phagosomes purified from THP-1 cells exhibit a high level of purity with relatively little extraneous material (Fig. 2*C*) and a high level of enrichment over the PNS starting material (Fig. 2*B*). In addition, we performed a quantitative analysis of the phagosomal purity of our 3-day BCG phagosomes by using the radioisotopic mixing method described by Chakraborty

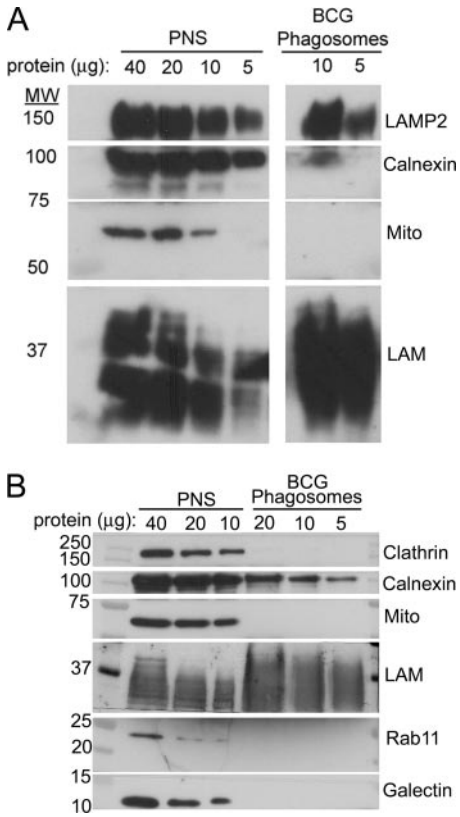


FIG. 3. **Analysis of 3-day purified BCG phagosomes from THP-1 cells by Western immunoblotting.** *A*, comparison of levels of LAMP-2, calnexin, 60-kDa mitochondrial antigen, and mycobacterial LAM. Samples containing 5–40 $\mu$g of protein from the PNS or BCG phagosomes prepared from THP-1 cells 3 days postinfection were analyzed by Western immunoblotting. Whereas LAMP-2 and mycobacterial LAM are enriched on the BCG phagosomes relative to the amount present in the PNS per $\mu$g of protein, calnexin is present at a markedly reduced level, and the 60-kDa mitochondrial antigen (*Mito*) is not detected in the purified BCG phagosome fraction. *B*, comparison of levels of clathrin, calnexin, mitochondrial antigen (*Mito*), LAM, Rab-11, and galectin-1. A separate Western immunoblot experiment demonstrates the enrichment of LAM in the BCG phagosome preparation and the persistence of low levels of calnexin relative to the levels present in the PNS. In contrast, clathrin, the mitochondrial antigen, Rab-11, and galectin-1 are detected in the PNS but not in the BCG phagosome preparation.

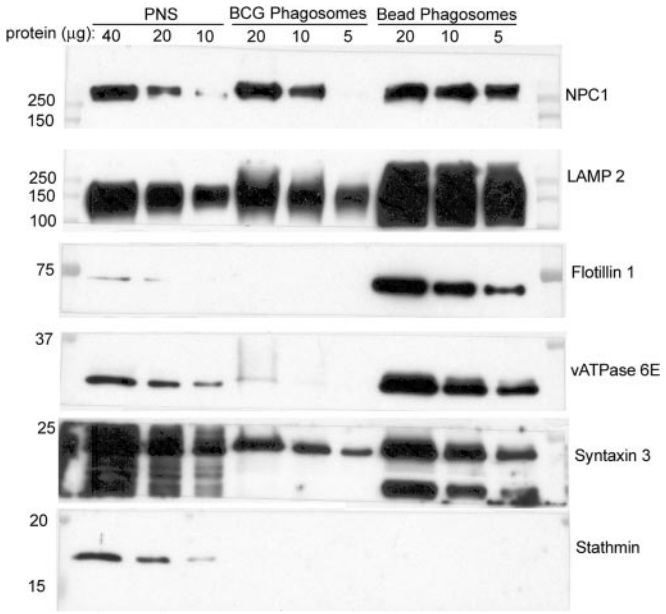


FIG. 4. **Analysis of 3-day purified BCG phagosomes, latex bead phagosomes, and PNS by Western immunoblotting.** Samples containing 5–40 $\mu$g of protein from the PNS, purified BCG phagosomes, or purified latex bead phagosomes prepared from THP-1 cells 3 days postinfection were analyzed by Western immunoblotting. NPC1, LAMP-2, and syntaxin 3 are enriched on the latex bead phagosomes relative to the levels observed on BCG phagosomes and the PNS. Flotillin-1 and the vATPase are greatly enriched on the latex bead phagosome and relatively scarce on the BCG phagosome. The cytoskeletal protein stathmin, on the other hand, is detected in the PNS but not in the latex bead or BCG phagosome preparations.

*et al.* (18) and obtained calculated purities of 82.5 and 92%, respectively.

To analyze the degree to which selected proteins are associated with or excluded from the BCG and latex bead phagosomes, we loaded SDS-PAGE gels with known amounts of protein from either the PNS or purified phagosomal preparations and analyzed the proteins present in the sample by Western immunoblotting. The purified BCG phagosomes exhibited an enrichment in mycobacterial LAM, a strong presence of LAMP-2, the absence of the mitochondrial 60-kDa marker, and a relative depletion in calnexin relative to the levels found in the PNS (Fig. 3*A*). Plasma membrane-associated proteins galectin-1 and clathrin were abundant in the PNS but not detected by Western immunoblotting in the BCG phagosome preparation (Fig. 3*B*). Rab-11, a marker of recycling endosomes, was detected in the PNS but was relatively depleted in the BCG phagosome preparation (Fig. 3*B*). We also compared the relative enrichment or depletion of selected markers on BCG phagosomes and latex bead phagosomes isolated from THP-1 macrophages at 3 days postinfection by analyzing equivalent amounts of phagosomal proteins by Western immunoblotting (Fig. 4). Whereas NPC1 and LAMP-2 were greatly enriched on the latex bead phagosomes, their relative abundance on BCG phagosomes was similar to that in the PNS. Whereas flotillin-1 and vATPase 6E were greatly enriched on latex bead phagosomes (relative to the PNS), they were markedly depleted on BCG phagosomes (Fig. 4). The membrane trafficking protein syntaxin 3 also was depleted on BCG phagosomes relative to its abundance on latex bead phagosomes and in the PNS (Fig. 4). The cytoskeletal protein stathmin was present in the PNS but was undetectable by Western immunoblotting in both the BCG and latex bead phagosome preparations (Fig. 4).

### *Proteomics Analysis of BCG Phagosomes*

Proteins present in BCG phagosomes and latex bead phagosomes purified from THP-1 cells infected for 3 h, 1 day, 3

days, or 5 days were separated by SDS-PAGE on gradient gels, the gel slices were digested with trypsin, and the resulting peptides were extracted and analyzed by nano-HPLC-MS/MS. The constituent proteins were identified by comparison against the human genome. Because of the complexity of these mixtures even after one-dimensional gel separations and to obtain an in-depth coverage of the proteins in these preparations, we subjected the trypsin-digested gel slices to HPLC-MS/MS analysis. A total of 475 different human proteins were identified in at least one of the BCG or latex bead phagosome preparations by HPLC-MS/MS analysis (supplemental Table 1). In addition, we identified 14 mouse proteins on one-dimensional and two-dimensional gels using the same methods in a limited analysis of BCG phagosomes isolated 1 day postinfection of J774 macrophages (supplemental Fig. 1 and Tables 2 and 3). A total of 447 human proteins were identified in one or more of the five BCG phagosome preparations, and a total of 289 were identified in one or more of the three latex bead phagosome preparations; 260 proteins were also identified one or more times in both BCG and latex bead phagosome preparations. To assess the consistency with which individual proteins were identified in the BCG phagosome preparations, we ranked each protein based on how often it was detected in the five BCG preparations (*i.e.* four time points with one independent biological replicate of the 3-day time point; supplemental Table 1). We identified 32 host proteins at all four time points in all five of the BCG phagosome preparations (supplemental Table 1). All 32 of these were also identified in at least one latex bead phagosome preparation, and 16 were identified in all three of the latex bead phagosome preparations. We identified 98 proteins in at least four BCG phagosome preparations of which all but 13 were found in at least one latex bead phagosome preparation (Table I, first 13 proteins), and we identified 178 proteins in at least three of the five BCG phagosome preparations of which all but 32 were found in at least one of the latex bead phagosome preparations (Table I, all proteins). These data indicate a high level of concordance for the proteins present in the BCG and latex bead phagosome preparations. Because only the 3-day time point was assessed more than once, we did not attempt to evaluate changes in phagosome composition over time; instead we used the data to identify a set of proteins that were consistently detected on the BCG phagosome across multiple preparations.

Although our proteomics analysis of BCG phagosomes and latex bead phagosomes indicate that there are more proteins in common than not for these two compartments, the distinctions between the two compartments may reflect important differences in cell biology. Included among the 32 proteins present in BCG phagosomes and undetected in latex bead phagosomes (Table I) were (*a*) proteins involved in membrane trafficking, vesicle-trafficking protein Sec22b, charged multivesicular body protein 4b (CHMP4b), Ras-related proteins Rab-14, Rab-6A, and Ral-A/Ral-B; (*b*) membrane proteins CD44 and intercellular adhesion molecule 1; (*c*) proteins thought to be involved in signal transduction or regulation of the cytoskeleton, Ras GTPase-activating-like protein IQGAP1, stress-induced phosphoprotein 1, septin-7, and band 4.1-like protein 3; and (*d*) the macrophage-secreted protein, macrophage migration-inhibitory factor, and the putative secreted protein FAM3C (Table I). Attempts to validate many of the proteins listed in Table I by Western immunoblotting were unsuccessful because of problems with a lack of sensitivity and specificity of the available antibodies (*i.e.* the available antibodies were either non-reactive with the proteins on blots, or they had excessive cross-reactivity with mycobacterial antigens). However, we confirmed the presence of IQGAP1 on *M. bovis* BCG phagosomes but not latex bead phagosomes by Western immunoblotting (supplemental Fig. 3), and we confirmed by immunofluorescence microscopy the differential presence of FAM3C on *M. bovis* BCG phagosomes but not latex bead phagosomes (supplemental Fig. 4).

Of the 289 proteins identified in at least one of the latex bead phagosome preparations, 34 were identified in all three latex bead phagosome preparations. All 34 of these were detected in at least one BCG phagosome preparation, and 29 were identified in at least four of the five BCG phagosome preparations (supplemental Table 1), demonstrating again the high concordance of proteins on the latex bead and BCG phagosome preparations. Of 104 host proteins found in at least two of the three latex bead phagosome preparations, only two were not found in any of the BCG phagosome preparations: the lysosomal enzymes $\beta$-galactosidase and sialate *O*-acetyltransferase. We confirmed by immunofluorescence microscopy that $\beta$-galactosidase was present on latex bead phagosomes but not on BCG phagosomes at 3-days postinfection in THP-1 cells (supplemental Fig. 4). In addition, the lysosomal hydrolase glucosylceramidase was found in two of the latex bead phagosome preparations (3 h and 5 day) but only in the 3-h BCG phagosome preparation. The lower representation or absence of the lysosomal enzymes glucosylceramidase, $\beta$-galactosidase, and sialate *O*-acetyltransferase may reflect a lesser degree of fusion of the BCG phagosome with lysosomes relative to the latex bead phagosome. Of the 104 host proteins identified in at least two of the three latex bead phagosome preparations, 61 were also identified in at least four of the five BCG phagosome preparations (Table II).

Noteworthy proteins identified in the BCG phagosome included the following.

*Endosomal-Lysosomal Proteins*—Among the proteins found in at least four of the five BCG phagosome preparations and at least two of the three latex bead phagosome preparations were several well known endolysosomal proteins: the lysosomal membrane glycoproteins CD63, LAMP-1, LAMP-2, and lysosome membrane protein 2; subunit B of the vATPase; cathepsin D; cathepsin Z; palmitoyl-protein thioesterase; lysosomal acid phosphatase; *N*-acetylglucosamine-6-sulfat-

TABLE I

*Proteins identified in the majority of BCG phagosome preparations that were not identified in any latex bead phagosome preparations*

No. BCG+ indicates the number of BCG phagosome preparations (out of five total) in which the indicated protein was identified. PM, plasma membrane; HA, hyaluronic acid; LFA-1, lymphocyte function associated antigen-1.

| Protein identified | Swiss-Prot accession no. | Reported location[a] | Physiological function[a] | No. BCG+ | Spectral/peptide counts[b] | | | | |
|---|---|---|---|---|---|---|---|---|---|
| | | | | | 3 h | 1 day | 3 days (a) | 3 days (b) | 5 days |
| CD44 antigen | P16070 | PM | HA receptor | 4 | 0 | 1/1 | 1/1 | 1/1 | 2/2 |
| Erlin-2 (SPFH domain-containing protein 2) | O94905 | ER membrane, PM | Lipid raft-associated | 4 | 3/3 | 0 | 5/1 | 1/1 | 3/2 |
| Golgi apparatus protein 1 (E-selectin ligand 1) | Q92896 | Golgi and PM | Binds fibroblast growth factor and E-selectin | 4 | 0 | 2/2 | 4/4 | 24/24 | 11/11 |
| Intercellular adhesion molecule 1 | P05362 | PM | Ligand for LFA-1 protein | 4 | 0 | 1/1 | 2/2 | 3/3 | 1/1 |
| Protein FAM3C | Q92520 | Putative macrophage-secreted protein | Unknown; member of cytokine-like gene family; may be involved in cell differentiation and proliferation during embryogenesis | 4 | 0 | 4/4 | 2/2 | 4/4 | 4/4 |
| Ras GTPase-activating-like protein IQGAP1 | P46940 | Membrane | Integrates $Ca^{2+}$/calmodulin and Cdc42 signaling | 4 | 0 | 3/3 | 5/4 | 9/9 | 14/14 |
| Ras-related protein Rab-6A | P20340 | Golgi | Golgi to ER traffic | 4 | 0 | 2/2 | 2/2 | 7/7 | 6/6 |
| Stress-induced-phosphoprotein 1 | P31948 | Cytoplasm, nucleus | Mediates the association of chaperones Hsc70 and Hsc90 | 4 | 0 | 6/6 | 2/2 | 5/5 | 8/8 |
| Transmembrane emp24 domain-containing protein 9 | Q9BVK6 | ER membrane | Unknown | 4 | 0 | 1/1 | 1/1 | 2/2 | 1/1 |
| Tubulin $\alpha$-1C chain | Q9BQE3 | Cytoplasm | Cytoskeleton | 4 | 0 | 7/7 | 3/3 | 7/7 | 2/2 |
| Tubulin $\beta$ chain | P07437 | Cytoplasm | Cytoskeleton | 4 | 0 | 13/12 | 12/11 | 12/12 | 4/4 |
| Tumor protein D54 | O43399 | Unknown | Unknown | 4 | 0 | 1/1 | 2/2 | 3/3 | 1/1 |
| Very long-chain-specific acyl-CoA dehydrogenase, mitochondrial | P49748 | Mitochondrion | Fatty acid $\beta$-oxidation system | 4 | 0 | 4/4 | 4/4 | 1/1 | 2/2 |
| ADP/ATP translocase 2 | P05141 | Mitochondrion | ATP/ADP translocation | 3 | 4/4 | 3/3 | 1/1 | 0 | 0 |
| $\alpha$-Mannosidase 2 | Q16706 | Golgi | *N*-Glycosylation | 3 | 0 | 2/2 | 0 | 6/6 | 12/12 |
| Band 4.1-like protein 3 | Q9Y2J2 | Cytoplasm | Links membrane to cytoskeleton | 3 | 0 | 0 | 1/1 | 1/1 | 2/2 |
| Charged multivesicular body protein 4b | Q9H444 | Cytoplasm, endosome | MVB formation and sorting of endosomal cargo proteins into MVBs | 3 | 0 | 0 | 5/3 | 2/2 | 1/1 |
| Glutamate dehydrogenase 1, mitochondrial | P00367 | Mitochondrion | Oxidative deamination of glutamate to $\alpha$-ketoglutarate | 3 | 4/3 | 2/2 | 2/2 | 0 | 0 |
| Guanine nucleotide-binding protein $G_i/G_s/G_t$ subunit $\beta$-1 | P62873 | Membrane | Transmembrane signaling | 3 | 3/3 | 0 | 0 | 2/2 | 2/2 |
| Integrin $\alpha$5 | P08648 | PM | Receptor for fibronectin and fibrinogen, present in endocytic pathway (36) | 3 | 1/1 | 3/3 | 1/1 | 0 | 0 |
| Nucleobindin-1 | Q02818 | Golgi, cytoplasm, membrane | Calcium homeostasis | 3 | 0 | 3/3 | 0 | 6/6 | 8/8 |
| Platelet endothelial cell adhesion molecule | P16284 | PM | Cell adhesion; signal transduction | 3 | 0 | 0 | 5/5 | 4/4 | 5/5 |
| Ras-related protein Rab-14 | P61106 | Membrane | Vesicular trafficking | 3 | 0 | 1/1 | 1/1 | 2/2 | 0 |
| Septin-7 | Q16181 | Cytoplasm | GTPase; associates with actin stress fibers; involved in cytokinesis and exocytosis | 3 | 0 | 0 | 2/2 | 2/2 | 4/4 |

TABLE I—*continued*

| Protein identified | Swiss-Prot accession no. | Reported location[a] | Physiological function[a] | No. BCG+ | Spectral/peptide counts[b] | | | | |
|---|---|---|---|---|---|---|---|---|---|
| | | | | | 3 h | 1 day | 3 days (a) | 3 days (b) | 5 days |
| Synaptic vesicle membrane protein VAT-1 homolog | Q99536 | Membrane | Unknown; ATPase with homology to oxidoreductase and ξ-crystallin | 3 | 2/2 | 0 | 0 | 1/1 | 2/2 |
| Vacuolar proton pump subunit C 1 | P21283 | Intracellular compartments, endosome-lysosome | Compartment acidification | 3 | 6/6 | 0 | 0 | 1/1 | 1/1 |
| Vesicle-trafficking protein Sec22b | O75396 | ER-Golgi-intermediate compartment, melanosome | ER to Golgi targeting and fusion | 3 | 0 | 0 | 2/2 | 2/2 | 3/3 |
| 60 S ribosomal protein L35 | P42766[c] | Cytoplasm | Protein synthesis | 3 | 0 | 1/1 | 0 | 1/1 | 1/1 |
| 60 S ribosomal protein L8 | P62917[c] | Cytoplasm | Protein synthesis | 3 | 0 | 0 | 1/1 | 1/1 | 1/1 |
| Macrophage migration-inhibitory factor | P14174[c] | Macrophage-secreted protein | Proinflammatory immune modulator | 3 | 0 | 1/1 | 1/1 | 1/1 | 0 |
| Ras-related protein Ral-B[d] | P11234[c] | Membrane | Signal transduction; regulation of exocytosis; activation of IκB kinase TBK1 | 3 | 1/1 | 0 | 0 | 1/1 | 1/1 |
| Translocon-associated protein subunit α | P43307[c] | ER | Binds $Ca^{2+}$ to ER membrane; regulates retention of ER-resident proteins | 3 | 1/1 | 0 | 1/1 | 0 | 1/1 |

[a] Except where indicated by referenced citation, "Reported location" and "Physiological function" are abstracted from the Swiss-Prot database.

[b] Spectral counts refer to all acquired precursor ions for a particular protein, whereas peptide counts only list the number of unique peptide sequences observed per protein (for correlation of spectral counts to the relative protein concentration see Liu *et al.* (83)). For BCG, these are listed for 3 h, 1 days, 3 days (a), 3 days (b), and 5 days, respectively. 3 days (a) and 3 days (b) are biological replicates.

[c] Proteins identified by single peptide assignments.

[d] Ral-B (P11234) could not be differentiated from Ral-A (also see supplemental Table 1); 78% sequence identity between Ral-B and Ral-A (P11233).

TABLE II

*Proteins shared by BCG and latex bead phagosomes (proteins identified in at least four of five BCG and at least two of three latex bead phagosome preparations)*

PM, plasma membrane; PKC, protein kinase C.

| Protein identified | Swiss-Prot accession no. | No. BCG[a] | No. bead[b] | Spectral/peptide count[c] | | Reported location[d] | Physiological function[d] |
|---|---|---|---|---|---|---|---|
| | | | | BCG | Bead | | |
| 60-kDa heat shock protein, mitochondrial | P10809 | 5 | 3 | 9, 19, 15, 2, 18/ 9, 19, 14, 2, 18 | 12, 16, 5/ 12, 16, 5 | Mitochondrion, secretory granules | Chaperone; extramitochondrial localization reported (75–77) |
| 78-kDa glucose-regulated protein | P11021 | 5 | 3 | 5, 16, 6, 8, 13/ 5, 16, 6, 8, 13 | 5, 8, 16/ 5, 8, 16 | ER, melanosome | Chaperone; member of heat shock protein 70 family |
| ATP synthase subunit $\alpha$ | P25705 | 5 | 3 | 13, 12, 2, 4, 6/ 13, 12, 2, 4, 6 | 9, 7, 2/ 9, 7, 2 | Mitochondrion inner membrane | Ion transport; generation of ATP |
| Aminopeptidase N | P15144 | 5 | 3 | 13, 8, 31, 20, 21/ 13, 8, 20, 20, 21 | 9, 17, 9/ 9, 12, 9 | PM | Protein degradation |
| Calnexin | P27824 | 5 | 3 | 1, 2, 2, 1, 2/ 1, 2, 2, 1, 2 | 1, 1, 3/ 1, 1, 3 | ER | Chaperone; protein synthesis and folding |
| Endoplasmin | P14625 | 5 | 3 | 4, 11, 10, 14, 13/ 4, 11, 10, 14, 13 | 9, 10, 14/ 8, 9, 13 | ER | Protein synthesis and folding |
| Integrin $\beta$2 | P05107 | 5 | 3 | 5, 7, 8, 6, 12/ 5, 7, 8, 6, 12 | 3, 2, 2/ 3, 2, 2 | PM | Cell surface adhesion glycoprotein |
| Lysosome membrane protein 2 | Q14108 | 5 | 3 | 15, 3, 9, 12, 3/ 13, 3, 9, 12, 3 | 12, 5, 2/ 11, 5, 2 | Lysosome | Lysosomal receptor; scavenger receptor class B member 2 |
| Lysosome-associated membrane glycoprotein 1 | P11279 | 5 | 3 | 4, 2, 4, 6, 3/ 4, 2, 3, 6, 3 | 4, 3, 2/ 4, 3, 2 | Lysosome, endosome, PM | Presents carbohydrate ligands to selectins |
| Lysosome-associated membrane glycoprotein 2 | P13473 | 5 | 3 | 3, 1, 4, 2, 2/ 3, 1, 3, 2, 2 | 3, 5, 1/ 2, 3, 1 | Lysosome, endosome, PM | Protects lysosomal membrane from autodigestion |
| Moesin | P26038 | 5 | 3 | 3, 8, 3, 9, 12/ 3, 8, 3, 9, 12 | 4, 7, 14/ 4, 7, 14 | Cytoplasm | Connections of membrane to cytoskeleton |
| Peroxiredoxin-1 | Q06830 | 5 | 3 | 1, 2, 2, 6, 8/ 1, 2, 2, 5, 7 | 2, 1, 11/ 2, 1, 10 | Cytoplasm, melanosome | Redox regulation; detoxification |
| Protein-disulfide isomerase | P07237 | 5 | 3 | 3, 2, 5, 9, 7/ 3, 2, 5, 9, 7 | 2, 7, 11/ 2, 7, 11 | ER | Disulfide bond rearrangement |
| Protein-disulfide isomerase A3 | P30101 | 5 | 3 | 1, 2, 10, 9, 10/ 1, 2, 10, 9, 10 | 2, 7, 7/ 2, 6, 7 | ER | Disulfide bond rearrangement |
| Putative elongation factor 1$\alpha$-like 3 | Q5VTE0 | 5 | 3 | 2, 5, 4, 3, 5/ 2, 5, 4, 3, 5 | 4, 8, 7/ 4, 7, 5 | Cytoplasm | Protein biosynthesis (by similarity) |
| Ras-related protein Rab-5C | P51148 | 5 | 3 | 4, 4, 5, 8, 3/ 4, 4, 5, 7, 3 | 4, 6, 1/ 4, 5, 1 | Early endosome | Vesicular trafficking |
| Acid ceramidase | Q13510 | 5 | 2 | 2, 1, 2, 2, 2/ 2, 1, 2, 2, 2 | 2, 2, 0/ 2, 2, 0 | Lysosome | Hydrolyzes ceramide into sphingosine and free fatty acid |
| CD63 antigen | P08962 | 5 | 2 | 2, 4, 2, 3, 2/ 2, 4, 2, 3, 2 | 3, 4, 0/ 3, 3, 0 | Late endosome-lysosome | Unknown; may regulate transport of other proteins |
| Coronin-1A | P31146 | 5 | 2 | 2, 1, 3, 3, 2/ 2, 1, 3, 3, 2 | 0, 4, 4/ 0, 3, 4 | Cytoplasm | Cytoskeleton component; important in membrane invaginations, protrusions, and cell locomotion |
| Erythrocyte band 7 integral membrane protein (stomatin) | P27105 | 5 | 2 | 1, 2, 2, 3, 4/ 1, 2, 2, 3, 4 | 6, 6, 0/ 6, 6, 0 | PM, melanosome | Regulates cation conductance; associates with actin and lipid rafts |
| Flotillin-1 | O75955 | 5 | 2 | 3, 1, 7, 1, 1/ 3, 1, 7, 1, 1 | 4, 9, 0/ 3, 9, 0 | PM, phagosomal membrane | Lipid rafts; clathrin-independent endocytosis; formation of caveolae or caveolae-like vesicles |

TABLE II—*continued*

| Protein identified | Swiss-Prot accession no. | No. BCG[a] | No. bead[b] | Spectral/peptide count[c] | | Reported location[d] | Physiological function[d] |
|---|---|---|---|---|---|---|---|
| | | | | BCG | Bead | | |
| Fructose-bisphosphate aldolase A | P04075 | 5 | 2 | 3, 8, 5, 14, 15/ 3, 8, 5, 12, 15 | 4, 0, 14/ 4, 0, 13 | Cytoplasm | Metabolism; interacts with cytoskeleton (78) |
| Heat shock protein HSP90-$\beta$ | P08238 | 5 | 2 | 5, 10, 16, 22, 10/ 5, 10, 14, 22, 10 | 3, 0, 18/ 3, 0, 17 | Cytoplasm, melanosome | Chaperone |
| Proactivator polypeptide (prosaposin) | P07602 | 5 | 2 | 4, 1, 2, 4, 1/ 4, 1, 2, 4, 1 | 3, 3, 0/ 3, 3, 0 | Lysosome | Sphingolipid degradation |
| Ras-related protein Rab-11B | Q15907 | 5 | 2 | 1, 2, 2, 1, 1/ 1, 2, 2, 1, 1 | 1, 1, 0/ 1, 1, 0 | Recycling endosome, PM | Regulation of endosomal recycling |
| Stress-70 protein, mitochondrial | P38646 | 5 | 2 | 12, 3, 8, 5, 4/ 12, 3, 8, 5, 4 | 2, 6, 0/ 2, 6, 0 | Mitochondrion, cell surface | Chaperone; control of cell proliferation and cellular aging |
| Thioredoxin-dependent peroxide reductase, mitochondrial | P30048 | 5 | 2 | 2, 1, 1, 1, 1/ 1, 1, 1, 1, 1 | 1, 1, 0/ 1, 1, 0 | Mitochondrion, early endosome | Redox regulation; presence in endosomes reported (79) |
| Vacuolar ATP synthase subunit B | P21281 | 5 | 2 | 10, 2, 3, 7, 2/ 10, 2, 3, 7, 2 | 8, 15, 0/ 8, 11, 0 | Endosome-lysosome | Compartment acidification |
| Actin, cytoplasmic 1 | P60709 | 4 | 3 | 5, 0, 16, 16, 49/ 5, 0, 12, 13, 16 | 3, 2, 18/ 3, 2, 13 | Cytoplasm | Cytoskeleton |
| Annexin A2 | P07355 | 4 | 3 | 5, 0, 4, 9, 9/ 5, 0, 4, 9, 9 | 15, 8, 5/ 13, 6, 5 | Secreted, extracellular matrix, basement membrane | May cross-link PM phospholipids with actin cytoskeleton and be involved in exocytosis |
| Brain acid-soluble protein 1 | P80723 | 4 | 3 | 4, 0, 6, 3, 4/ 4, 0, 5, 3, 4 | 3, 5, 1/ 3, 5, 1 | Membrane | Signaling; regulation of actin dynamics; present in lipid rafts; has calmodulin binding site; is substrate for PKC |
| Cathepsin D | P07339 | 4 | 3 | 6, 0, 5, 8, 9/ 5, 0, 5, 8, 8 | 9, 15, 5/ 8, 11, 5 | Lysosome | Protein degradation |
| Glyceraldehyde-3-phosphate dehydrogenase | P04406 | 4 | 3 | 2, 0, 3, 3, 7/ 2, 0, 3, 3, 7 | 3, 3, 5/ 3, 3, 5 | Cytoplasm, membrane-associated | Glycolysis; membrane fusion; microtubule bundling; phosphotransferase activity; nuclear RNA export; DNA replication and DNA repair (80) |
| Heat shock cognate 71-kDa protein | P11142 | 4 | 3 | 6, 0, 9, 22, 8/ 6, 0, 9, 22, 8 | 3, 5, 11/ 3, 5, 11 | Cytoplasm, melanosome | Chaperone |
| Palmitoyl-protein thioesterase 1 | P50897 | 4 | 3 | 3, 0, 3, 3, 4/ 3, 0, 3, 3, 4 | 4, 6, 1/ 4, 5, 1 | Lysosome | Lipoprotein degradation |
| Plastin-2 | P13796 | 4 | 3 | 0, 10, 2, 12, 14/ 0, 10, 2, 12, 14 | 2, 3, 11/ 2, 3, 11 | Cytoplasm | Cytoskeleton |
| Ras-related protein Rab-7A | P51149 | 4 | 3 | 2, 0, 5, 4, 7/ 2, 0, 5, 4, 7 | 3, 3, 2/ 3, 3, 2 | Late endosome | Late endosomal transport; phagosome maturation |
| Vacuolar ATP synthase catalytic subunit A | P38606 | 4 | 3 | 3, 0, 1, 7, 4/ 3, 0, 1, 7, 4 | 4, 12, 1/ 4, 10, 1 | Endosome-lysosome | Compartment acidification |
| Vimentin | P08670 | 4 | 3 | 0, 5, 9, 2, 5/ 0, 5, 9, 2, 5 | 7, 8, 1/ 7, 8, 1 | Cytoplasm | Cytoskeleton; intermediate filament |
| Voltage-dependent anion-selective channel protein 1 | P21796 | 4 | 3 | 4, 0, 2, 5, 7/ 4, 0, 1, 5, 7 | 2, 3, 5/ 2, 3, 5 | Mitochondrion, PM | Channel for small hydrophilic molecules; present in secretory pathway and PM (81) |
| Voltage-dependent anion-selective channel protein 2 | P45880 | 4 | 3 | 2, 0, 3, 2, 5/ 2, 0, 3, 2, 5 | 2, 1, 2/ 2, 1, 2 | Mitochondrion | Channel for small hydrophilic molecules |

TABLE II—*continued*

| Protein identified | Swiss-Prot accession no. | No. BCG[a] | No. bead[b] | Spectral/peptide count[c] | | Reported location[d] | Physiological function[d] |
|---|---|---|---|---|---|---|---|
| | | | | BCG | Bead | | |
| 10-kDa heat shock protein, mitochondrial | P61604 | 4 | 2 | 6, 6, 4, 4, 0/ 6, 5, 4, 4, 0 | 3, 5, 0/ 3, 5, 0 | Mitochondrion and non-mitochondrial sites | Co-chaperone for Hsp60 in the protein folding process; also identified in non-mitochondrial sites, including secretory granules (82) |
| 40 S ribosomal protein SA (laminin receptor-1) | P08865 | 4 | 2 | 0, 1, 2, 3, 5/ 0, 1, 1, 3, 5 | 0, 1, 3/ 0, 1, 3 | Cytoplasm | Protein synthesis; cell adhesion |
| ADP-ribosylation factor-like protein 8B[e] | Q9NVJ2 | 4 | 2 | 3, 1, 1, 1, 0/ 3, 1, 1, 1, 0 | 2, 1, 0/ 2, 1, 0 | Late endosome-lysosome | Endosome and lysosome motility |
| $\alpha$-Enolase | P06733 | 4 | 2 | 0, 1, 2, 6, 7/ 0, 1, 2, 6, 7 | 1, 0, 3/ 1, 0, 3 | Cytoplasm, PM, myofibril, sarcomere | Carbohydrate degradation; glycolysis; promotes vacuole fusion in yeast; may also function as a plasminogen receptor and activator on the PM |
| Cathepsin Z | Q9UBR2 | 4 | 2 | 3, 0, 1, 3, 2/ 3, 0, 1, 3, 2 | 2, 2, 0/ 2, 2, 0 | Lysosome | Carboxydipeptidase |
| Cofilin-1 | P23528 | 4 | 2 | 1, 2, 0, 2, 1/ 1, 2, 0, 2, 1 | 1, 0, 2/ 1, 0, 2 | Cytoplasm | Controls actin polymerization |
| Gelsolin | P06396 | 4 | 2 | 0, 1, 2, 8, 5/ 0, 1, 2, 8, 5 | 1, 0, 7/ 1, 0, 7 | Cytoplasm | Cytoskeleton |
| Hypoxia up-regulated protein 1 | Q9Y4L1 | 4 | 2 | 0, 2, 1, 2, 7/ 0, 1, 1, 2, 7 | 1, 0, 3/ 1, 0, 3 | ER lumen | Chaperone; induced by hypoxia |
| Lysosomal acid phosphatase | P11117 | 4 | 2 | 0, 1, 2, 1, 3/ 0, 1, 2, 1, 3 | 3, 5, 0/ 3, 5, 0 | Lysosome | Phosphate monoester hydrolysis |
| Lysosomal $\alpha$-glucosidase | P10253 | 4 | 2 | 2, 0, 2, 1, 1/ 2, 0, 2, 1, 1 | 3, 2, 0/ 3, 2, 0 | Lysosome | Glycogen degradation |
| Malate dehydrogenase, mitochondrial | P40926 | 4 | 2 | 11, 0, 6, 2, 8/ 11, 0, 5, 2, 8 | 5, 5, 0/ 5, 5, 0 | Mitochondrion | Glycolysis; tricarboxylic acid cycle |
| Myosin-9 | P35579 | 4 | 2 | 0, 14, 5, 29, 15/ 0, 14, 5, 29, 15 | 0, 7, 34/ 0, 7, 34 | Cytoplasm | Cytoskeleton |
| *N*-Acetylglucosamine-6-sulfatase | P15586 | 4 | 2 | 8, 1, 1, 3, 0/ 8, 1, 1, 3, 0 | 3, 2, 0/ 3, 2, 0 | Lysosome | Heparan sulfate/keratan sulfate hydrolysis |
| Nicastrin | Q92542 | 4 | 2 | 2, 1, 2, 2, 0/ 2, 1, 2, 2, 0 | 4, 3, 0/ 4, 3, 0 | Golgi, ER, PM, melanosome | Component of the $\gamma$-secretase complex |
| Protein-disulfide isomerase A6 | Q15084 | 4 | 2 | 0, 3, 1, 4, 6/ 0, 3, 1, 4, 6 | 1, 0, 2/ 1, 0, 2 | ER, ER-Golgi intermediate compartment, melanosome | Disulfide bond rearrangement |
| Ras-related protein Rab-21 | Q9UL25 | 4 | 2 | 1, 0, 2, 2, 1/ 1, 0, 2, 2, 1 | 1, 2, 0/ 1, 2, 0 | Endosomes | Controls traffic of $\beta$1 integrins |
| Sulfide:quinone oxidoreductase, mitochondrial | Q9Y6N5 | 4 | 2 | 2, 0, 6, 4, 6/ 2, 0, 6, 4, 6 | 2, 2, 0/ 2, 2, 0 | Mitochondrion | Hydrogen sulfide oxidation |

TABLE II—*continued*

| Protein identified | Swiss-Prot accession no. | No. BCG[a] | No. bead[b] | Spectral/peptide count[c] | | Reported location[d] | Physiological function[d] |
|---|---|---|---|---|---|---|---|
| | | | | BCG | Bead | | |
| Vacuolar proton pump subunit d 1 | P61421 | 4 | 2 | 3, 0, 6, 5, 1/ 3, 0, 5, 5, 1 | 4, 5, 0/ 4, 4, 0 | Intracellular compartments, endosome-lysosome | Compartment acidification |
| Citrate synthase, mitochondrial | O75390[f] | 4 | 2 | 1, 0, 1, 1, 1/ 1, 0, 1, 1, 1 | 1, 1, 0/ 1, 1, 0 | Mitochondrion | Carbohydrate metabolism; tricarboxylic acid cycle |
| Interferon-induced transmembrane protein 3[g] | Q01628[f] | 4 | 2 | 1, 1, 1, 1, 0/ 1, 1, 1, 1, 0 | 1, 1, 0/ 1, 1, 0 | PM, Golgi, integral membrane protein | Cell differentiation and homing; immune response |

[a] No. BCG indicates the number of BCG phagosome (out of five total) in which the indicated protein was identified.

[b] No. bead indicates the number of latex bead phagosome preparations (out of three total) in which the indicated protein was identified.

[c] Spectral counts refer to all acquired precursor ions for a particular protein, whereas peptide counts only list the number of unique peptide sequences observed per protein in the phagosome preparation (for correlation of spectral counts to the relative protein concentration see Liu *et al.* (83)). For BCG, these are listed for 3 h, 1 days, 3 days (a), 3 days (b), and 5 days, respectively. For latex beads, these are listed for 3 h, 3 days, and 5 days, respectively. The spectral counts for the 5 BCG phagosome preparations are listed together and are separated by a slash (/) from the peptide counts of the same 5 preparations, which are listed in the same order. The same is done for the spectral and peptide counts, respectively, for the 3 latex bead phagosome preparations.

[d] Reported location and physiological function are abstracted from the Swiss-Prot on-line database except where indicated by cited references.

[e] Arl 8B (Q9NVJ2) could not be differentiated from ARL 8A (Q96BM9) (also see supplemental Table 1) in three of four BCG phagosome preparations and one of two latex bead phagosome preparations.

[f] Proteins identified by single peptide assignments.

[g] Interferon-induced transmembrane protein 3 (Q01628) could not be differentiated from interferon-induced transmembrane protein 1 (P13164) or interferon-induced transmembrane protein 2 (Q01629) (also see supplemental Table 1).

ase; lysosomal $\alpha$-glucosidase; acid ceramidase; and prosaposin. We detected the mannose 6-phosphate receptor-binding protein (which interacts with mannose 6-phosphate receptor (M6PR)) in four of the five BCG phagosome preparations and in only one of the latex bead phagosome preparations, and we detected the cation-independent M6PR in two of the five BCG preparations but in none of the latex bead phagosome preparations. Association of the M6PR and the M6PR-binding protein with the BCG phagosome may reflect the BCG phagosome being in a less mature, late endosomal-like compartment as opposed to a phagolysosomal compartment.

*Multivesicular Body (MVB) and Exosome Pathway*—In addition to many classical components of the endosomal-lysosomal pathway, we also identified many components of the more recently described MVB-exosome pathway in both BCG and latex bead phagosomes. For example, we identified programmed cell death 6-interacting protein (Alix) in both the 3- and 5-day BCG phagosomes (supplemental Table 1). This protein interacts with CHMP4b to promote the formation of multivesicular bodies (31, 32). We identified CHMP4b in all 3- and 5-day BCG phagosomes but not in any of the latex bead phagosomes (supplemental Table 1). Alix has also been identified on latex bead phagosomes purified from mouse macrophages (14). To our knowledge, CHMP4b has not previously been identified in proteomics studies of phagosomes. MVBs are at the intersection of the endocytic pathway and the exosome pathway (33). Thus, interaction of the phagosome with the MVB allows antigen processing and presentation via the exosome pathway. Many additional proteins that have been identified as major constituents of exosomes (33–35) were present in the majority of our BCG phagosome preparations, including integrin $\beta$1 and $\beta$2; CD63; Rap-1B/Rap-1A; Rab-7; annexins A2, A4, and A5; Hsc70; Hsp90; actin; cofilin; tubulin; moesin; pyruvate kinase; enolase; elongation factor 1-$\alpha$; and 14-3-3. The presence of integrins in the endocytic pathway has been reported previously (36).

*Lipid Raft Proteins*—Lipid rafts and raft proteins (flotillin-1 and stomatin) are also enriched in the internal vesicles of MVBs and exosomes (33, 35). We identified the raft proteins flotillin-1 and stomatin in all of our BCG phagosome preparations and in two of the three latex bead phagosomes (Table II). In addition to the lipid raft proteins flotillin and stomatin, we also identified the lipid raft protein erlin-2 in four of five BCG phagosome preparations but in none of the latex bead phagosomes (Table I). Although flotillin (37) and stomatin (38) have been reported previously in association with phagocytic and endocytic pathways, erlin-2 was only recently identified as an ER-associated raft protein (39), and its presence in other intracellular compartments has not been reported.

*Signaling Proteins*—We identified many proteins involved in signaling by our proteomics analysis of the BCG phagosome. We identified ADP-ribosylation factor (Arf)-like protein 8b/8a (Arl 8b/8a) in the majority of BCG and latex bead phagosome

preparations (four of five and two of three, respectively), although it was not detected in either of the two 5-day phagosome preparations (Table II and supplemental Table 1). Arf 8b colocalizes with late endosomes and lysosomes, interacts with tubulin, and is involved in motility of lysosomes (40). Thus, Arl 8b/8a may also be involved in motility of both BCG and latex bead phagosomes.

We identified brain acid-soluble protein 1 (BASP1) in four of five BCG and all three latex bead phagosome preparations (Table II). BASP1, a myristoylated $Ca^{2+}$-dependent calmodulin-binding protein that is phosphorylated by protein kinase C, associates with cholesterol-rich lipid rafts and, in neuronal cells, is thought to regulate actin interactions with the plasma membrane (41). BASP1 has not been identified previously in association with phagosomes.

Heterotrimeric G-proteins are membrane-associated proteins composed of $\alpha$, $\beta$, and $\gamma$ subunits that together function in numerous signal transduction pathways. We identified one or more G-protein subunits (*e.g.* guanine nucleotide-binding protein $G_i$, $\alpha$-2 subunit (GNAI2), GNAI3, GNB1, GNG5, or GNG12) in the majority of our BCG and latex bead phagosome preparations, and we also identified the GNAI2 in our 1-day mouse J774 BCG phagosome preparation (supplemental Fig. 1 and Table 2). This protein, as well as other trimeric G-protein subunits, has also been identified in purified mouse J774 and *Drosophila* latex bead phagosomes (14, 42). Although the physiological role of G-proteins in mediating signal transduction events on the plasma membrane is well known (43), it is possible that they may also serve a similar function on the phagosomal membrane.

We identified the Ras GTPase-activating-like protein IQGAP1 in all of our BCG phagosome preparations except for the 3-h phagosome preparation, but we did not detect this protein in any of the latex bead phagosome preparations (Table I). Similarly, IQGAP1 was not identified in prior reports in latex bead phagosomes isolated from mouse or *Drosophila* macrophages, suggesting a true difference between the BCG phagosome and the latex bead phagosome. This signal transduction protein participates in multiple cellular signaling pathways, including interaction with Rac1, Cdc42, and $Ca^{2+}$/calmodulin to effect changes to the actin cytoskeleton (44).

We identified six members of the 14-3-3 family ($\beta/\alpha$, $\varepsilon$, $\eta$, $\gamma$, $\zeta/\delta$, and $\theta$) in the BCG phagosome preparation at days 3–5 (with $\beta/\alpha$, $\zeta/\delta$, and $\gamma$ identified in all of the 3–5-day BCG phagosome preparations), but no members of the family were identified in the 3-h or 1-day BCG phagosome preparations, and no members of the family were identified in latex bead phagosome preparations until day 5 (supplemental Table 1), suggesting that this protein family may be recruited more abundantly to BCG phagosomes than to latex bead phagosomes in THP-1 cells. However, the 14-3-3 family proteins have been identified by proteomics in latex bead phagosomes purified from mouse J774 macrophages (14). The 14-3-3 family proteins are involved in a large number of signaling pathways and interact with numerous proteins involved in vesicular transport (45). Similarly, we identified adenylyl cyclase-associated protein 1 (CAP1) in all of the BCG phagosomes at 1–5 days and in the 5-day latex bead phagosome preparation. CAP1 binds actin monomers and directly regulates filament dynamics (46). Thus, CAP1 may regulate the interaction of BCG and latex bead phagosomes with actin microfilaments.

*Rab and Rab-related Proteins*—We identified many Rab GTPase and Rab-related proteins in both the BCG and latex bead phagosome preparations. We identified Rab-5C in all of our BCG and latex bead phagosome preparations (Table II). We have previously demonstrated the presence of Rab-5C on *M. tuberculosis* phagosomes by immunoelectron microscopy (10).

We identified Rab-7A in four of our five BCG phagosome preparations and in all of our latex bead phagosome preparations (Table II). Rab-7A regulates vesicular traffic of late endosomes, and it has been detected on latex bead phagosomes of macrophages from mouse (14) and *Drosophila* (42). We have previously demonstrated the presence of Rab-7 on the *M. tuberculosis* phagosome by immunoelectron microscopy (9).

We identified Rab-11A/Rab-11B (Table II and supplemental Table 1) in all five of our BCG phagosome preparations and in two of our three latex bead phagosome preparations (all but day 5). Although Rab-11 is known for its role in endosomal recycling from a perinucleolar compartment to the plasma membrane, Rab-11 and its effector, Rab coupling protein, have been identified by immunofluorescence in patches on latex bead phagosomal membranes (47) and by proteomics in purified mouse J774 latex bead phagosomes (14). It has been proposed that Rab-11 may be involved in recycling of vesicles from the phagosome to the plasma membrane (47). Although we observed a relative depletion of Rab-11 by Western immunoblotting in our phagosome preparations relative to its abundance in the PNS (Fig. 3*B*), Rab-11 may still be present and of functional importance on the phagosomal membrane.

We identified Rab-1A/Rab-1B in four of our five BCG phagosome preparations and in the 3-day latex bead phagosome preparation (supplemental Table 1). Rab-1 also has been detected in latex bead phagosomes purified from *Drosophila* macrophages (42). Although Rab-1 is well known for regulation of transport between the ER-Golgi intermediate compartment and the Golgi compartment, Rab-1 has recently been demonstrated also to be involved in transport of vesicles from the ER-Golgi intermediate compartment toward the cell periphery (48). Thus, Rab-1 might also regulate the interaction of this ER-related compartment with the phagosome.

We identified Rab-6A in four of the five BCG phagosome preparations but in none of the latex bead phagosome preparations (Table I). However, Rab-6A has been reported in latex bead phagosomes from *Drosophila* (42). Rab-6A regulates traffic within Golgi stacks and between ER and Golgi, but it has also been shown to play a role in cytokinesis and in a

pathway that interacts with Rab-11 (49). The role of Rab-6A on phagosomes is not known.

We identified Rab-21 in four of five BCG phagosome preparations and in two of three latex bead phagosome preparations (Table II). Rab-21 was not reported in prior latex bead phagosome proteomics studies. Rab-21 is present on early endosomes (50) and has been shown to bind directly to integrins and to regulate the endocytic and exocytic traffic of integrins (51). We identified integrins as a component of the BCG phagosome, and thus Rab-21 may be involved in membrane trafficking of these molecules to or from the BCG phagosome.

We identified Rab-14 in three of five BCG phagosome preparations but in none of the latex bead phagosome preparations (Table I). This finding is consistent with a report by Kyei *et al.* (52), who found that Rab-14 was recruited to live but not dead *M. bovis* BCG phagosomes and that a dominant-negative form of Rab-14 promoted phagosomal maturation.

We identified Ral-B/Ral-A (based on single peptide identifications that could be assigned to either protein) in three of our five BCG phagosome preparations, but we did not detect this Ras GTPase in any of our latex bead phagosome preparations (Table I). It has not been reported in prior proteomics studies of latex bead phagosomes (14, 42). Ral-B has been shown to regulate exocytosis (53, 54), to play a role in organization of the actin cytoskeleton (55), and to be involved in signal transduction of toll-like receptors by activation of NF$\kappa$B via the I$\kappa$B kinase Tank binding kinase 1 (TBK1) (56). By immunofluorescence, we observed colocalization of endogenous Ral-B on the BCG phagosome.[2] In macrophages in which we overexpressed recombinant GFP-Ral-B, we observed colocalization of Ral-B with both BCG and latex bead phagosomes.[2] The function of Ral-B on the phagosomal membrane remains to be determined, but in view of its previously demonstrated roles, it could be important in regulating vesicular traffic or in signal transduction of toll-like receptors present on the phagosomal membrane.

We identified Rap-1A/Rap-1B in all of the latex bead phagosome preparations and in three of the five BCG phagosome preparations (supplemental Table 1). Rap-1A/Rap-1B have been identified by immunomicroscopy on late endosomes/lysosomes and phagosomes (57) and on exosomes (58) and by proteomics studies on latex bead phagosomes from mouse macrophages (14). Their function is not known, but there is evidence that Rap-1A has a role in initiation of the oxidative burst in neutrophils (59) and that Rap-1B regulates integrin signaling (60).

We identified Rab-guanine dissociation inhibitor (GDI) in two of five BCG phagosome preparations and also identified the Rho-GDP dissociation inhibitor in two of five BCG phagosome preparations but did not identify this protein in any of our latex bead phagosome preparations (supplemental Table 1). This finding complements the study of Fratti *et al.* (61), who reported persistence of GDI with BCG phagosomes but not latex bead phagosomes at early times after uptake and proposed that persistence of GDI on the mycobacterial phagosome was due to mycobacterial activation of p38 mitogen-activated protein kinase (MAPK) leading to phosphorylation of GDI. Greater levels of GDI on the BCG phagosome may displace EEA1 from the phagosomal membrane and impair phagosome maturation (61, 62).

*Secreted Proteins*—Apolipoproteins D and E are 21-kDa proteins synthesized and secreted by macrophages that are involved in cholesterol transport and catabolism. We identified either apolipoprotein D or apolipoprotein E on four of five BCG phagosome preparations and on all three latex bead phagosome preparations (supplemental Table 1). Others have also identified apolipoproteins in mouse J774 latex bead phagosomes (14). These proteins could be delivered to the BCG phagosome via either the endocytic or the secretory route. However, our mass spectrometry analysis of both apolipoproteins D and E indicated that they are of human rather than bovine origin, excluding the possibility that they were derived from the bovine serum in which the macrophages were cultured after the initial infection. Thus, it is likely that they are derived from the macrophage secretory pathway rather than of endocytic origin.

Whereas we identified apolipoproteins D and/or E in both early and late BCG phagosome preparations, we identified complement factors C3 and C9 only on the 3-h latex bead and BCG phagosome preparations, respectively (supplemental Table 1). Their presence only early after phagocytosis likely reflects adsorption or fixation of complement to the beads or bacteria prior to uptake.

We identified the secreted protein retinoid-inducible serine carboxypeptidase in three of five BCG phagosome preparations and in one latex bead phagosome preparation (supplemental Table 1). Kollman *et al.* (63) have shown that retinoid-inducible serine carboxypeptidase is delivered to endosomes/lysosomes by the M6PR.

*Proteins of Unknown Function*—We identified several proteins of unknown function in our BCG and latex bead phagosome preparations. Three proteins of unknown function that we identified on the majority of our BCG phagosome preparations but on none of the latex bead phagosome preparations are FAM3C, tumor protein D54, and synaptic vesicle amine transport membrane protein-1 (VAT-1) homolog. We identified FAM3C and tumor protein D54 in four of five BCG phagosome preparations and the VAT-1 homolog in three of five BCG phagosome preparations, but we identified none of these proteins in any of our latex bead phagosome preparations (Table I). FAM3C, tumor protein D54, and the VAT-1 homolog also were not identified in prior mouse or *Drosophila* latex bead phagosome preparations (14, 42). We also identified FAM3C by immunofluorescence on the BCG phagosome.

[2] B.-Y. Lee, D. L. Clemens, and M. A. Horwitz, unpublished data.

FAM3C has sequence similarity to human and mouse proteins from the cytokine-like gene family and has both a predicted signal sequence and a transmembrane domain (64). The function of FAM3C is unknown, and it is unclear whether it is a secreted or a membrane protein. Tumor protein D54 has been identified by MS-based proteomics studies in normal human astrocytes (65), in breast tumor cells (66), and in lipid droplets from lipolytically stimulated (but not unstimulated) adipocytes (67). No studies of its physiological function have been reported. The synaptic vesicle membrane protein VAT-1 homolog is a 41-kDa integral membrane protein with sequence similarity to the zinc-containing alcohol dehydrogenase family (68) and to the mammalian lens $\xi$-crystallin (69). It has been identified in human and mouse epithelial cells and shown to have ATPase activity and to be calcium-regulated (68, 70), but its function is otherwise unknown.

### *Evaluation of Flotillin-1 Location by Immunofluorescence*

Our proteomics analysis detected flotillin-1 in all of our BCG phagosome preparations and also in two of our latex bead phagosome preparations. Nevertheless, our Western immunoblots (Fig. 4) demonstrated that flotillin-1 was depleted in the BCG phagosome preparation relative to the latex bead phagosome preparation and the PNS. To evaluate further the association of flotillin-1 with mycobacterial phagosomes, we examined the degree of colocalization of flotillin-1 with *M. bovis* BCG and *M. tuberculosis* phagosomes in THP-1 cells. In accord with our Western immunoblotting data, *M. bovis* BCG phagosomes exhibited lower levels of flotillin-1 fluorescence than latex bead phagosomes at 3 days postinfection, although some heterogeneity in intensity of staining was observed (data not shown). To determine whether the heterogeneity in flotillin-1 immunofluorescence correlated with mycobacterial metabolic activity, we infected THP-1 macrophages with a recombinant *M. tuberculosis* (*Mtb*-iGFP) whose GFP expression is induced in response to IPTG (16) and examined GFP expression and flotillin-1 distribution 48 h postinfection. Only *M. tuberculosis* that are alive and metabolically active are able to express GFP in response to IPTG, which is added after infection of the macrophages. Using this system, we observed that *Mtb*-iGFP that fail to express GFP in response to IPTG reside within acidified compartments that fuse with Texas Red-dextran-labeled lysosomes, whereas *Mtb*-iGFP that do express GFP in response to IPTG reside in non-acidified compartments that do not fuse with Texas Red-dextran (16). In the current study, we observed an inverse correlation between GFP expression by the *Mtb*-iGFP and flotillin-1 immunofluorescence around the bacteria (Fig. 5, *A* and *B*). In contrast, killed *M. tuberculosis* and latex beads colocalized consistently with flotillin-1 immunofluorescence (Fig. 5*B*).

## DISCUSSION

We demonstrated a method for high level purification of BCG phagosomes by use of a combination of differential centrifugation and density gradient sedimentation on sucrose and iodixanol gradient media that is amenable to further molecular studies of the *M. bovis* BCG and *M. tuberculosis* phagosomes. We consistently observed a decrease in buoyant density of BCG and *M. tuberculosis* over time with growth in macrophages. The change in density most likely reflects a change in the density of the mycobacteria rather than a change in the macrophage contribution to the phagosome because electron microscopy analysis revealed a mixture of free bacteria (non-membrane-bound) as well as membrane-bound bacteria in the same density fractions. Moreover, phagosomes containing killed bacteria exhibited a heavier density than those containing live bacteria that have grown in macrophages for 1 or more days. The decrease in mycobacterial density probably reflects a change in lipid composition of the mycobacteria or an increase in the ratio of mycobacterial lipid to protein and carbohydrate that is induced by growth in macrophages.

Our proteomics analysis is an extremely sensitive method for study of the composition of the BCG phagosome and represents a first stage in the identification of proteins associated with the mycobacterial phagosome. An important strength of the technique is that it provides an unbiased assessment of the proteins present. However, confirmation of the presence of proteins identified by proteomics should be obtained by independent techniques such as immunofluorescence microscopy of intact macrophages infected with pathogenic mycobacteria. Hence, the list of proteins identified herein should be considered a list of candidate proteins present on the mycobacterial phagosome. Some of the proteins identified may reflect contaminants rather than proteins that are truly associated with the phagosome. Furthermore, although the proteins present on latex bead phagosomes and BCG phagosomes show considerable overlap with relatively few consistently detected proteins on only one or the other phagosome, the abundance of various proteins may differ greatly for latex bead and BCG phagosomes. For example, we identified flotillin-1 and the vATPase by mass spectrometry at all time points on both the latex bead and the BCG phagosome; however, by Western immunoblotting of phagosomes isolated 3 days postinfection, flotillin-1 and vATPase were enriched on the latex bead phagosomes but relatively scarce on the BCG phagosome. Consistent with this, by fluorescence microscopy, we observed weaker flotillin-1 immunofluorescence on BCG and *M. tuberculosis* phagosomes than on latex bead phagosomes, and use of an IPTG-inducible expression system showed that flotillin-1 colocalization with *M. tuberculosis* varied inversely with the metabolic activity of the mycobacteria. Flotillin-1 has been shown to be recruited to maturing

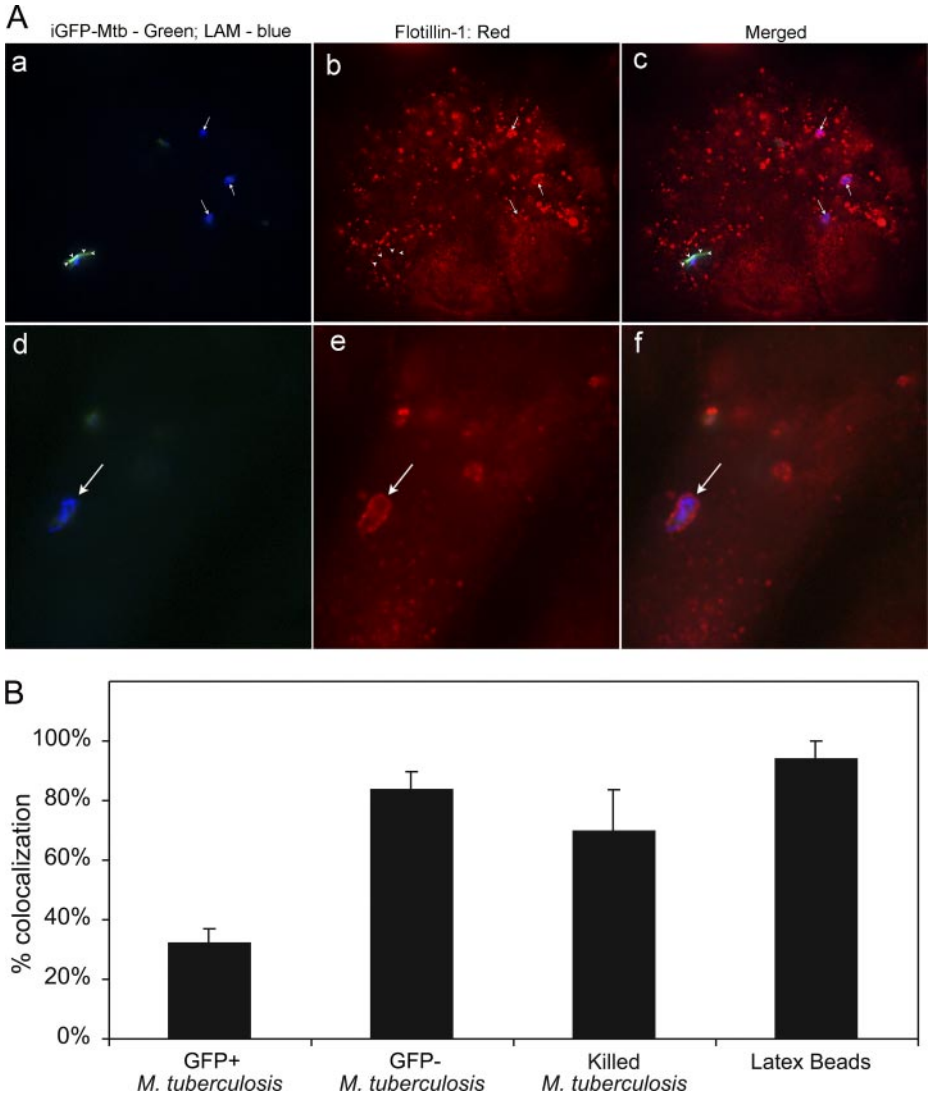


FIG. 5. **Flotillin-1 immunofluorescence on *M. tuberculosis* phagosomes in THP-1 cells correlates inversely with metabolic activity of mycobacteria.** *A*, metabolic activity of *Mtb*-iGFP was assessed by addition of IPTG after infection and visualization of green fluorescent protein expression at fixation 48 h postinfection (*a* and *d*), and *Mtb*-iGFP, independent of metabolic status, was visualized by blue fluorescence with aminomethylcoumarin-labeled anti-LAM antibody (*a* and *d*). Flotillin-1 distribution was visualized by staining with Texas Red-labeled anti-human flotillin-1 antibody (*b* and *e*). The merged color images are shown on the *right* (*c* and *f*). Metabolically inactive *Mtb*-iGFP (bacteria that do not express GFP after IPTG induction; *a–f*, *arrows*) consistently colocalized with flotillin-1 labeled with Texas Red (*arrows* indicating three bacteria in *b* and one bacterium in *e*). The metabolically active *Mtb*-iGFP (*a–c*, *arrowheads*) showed weaker and less consistent colocalization with flotillin-1 (*b*). *B*, quantitative assessment of flotillin-1 immunofluorescence demonstrates relatively low levels of colocalization of flotillin-1 on metabolically active *Mtb*-iGFP (*GFP+ M. tuberculosis*) compared with much higher levels of colocalization with inactive *Mtb*-iGFP (*GFP− M. tuberculosis*), formalin-killed *Mtb*-GFP (*Killed M. tuberculosis*), and latex beads at 48 h postinfection (and 46.5 h post-IPTG induction) in THP-1 cells. The experiment was performed twice with similar results. Values shown are means and error bars indicate S.D. for duplicate determinations for at least 40 bacteria or beads.

latex bead phagosomes (37) and to be a constituent of lipid rafts that also contain other proteins important to membrane trafficking and phagosome formation, including the $\alpha$- and $\beta$-subunits of heterotrimeric G proteins as well as subunits of the proton pump vATPase (71). Flotillin-1 may act as a scaffolding protein to organize lipid rafts containing the vATPase for delivery to the maturing phagosome. Thus, the relative scarcity of flotillin-1 on the BCG phagosome, as indicated in our Western immunoblotting and immunofluorescence studies, may be important in excluding the vATPase and resisting acidification.

Consistent with prior mass spectrometry-based proteomics analyses of phagosomes, we found multiple ER-associated proteins (including calnexin, endoplasmin, and protein-disulfide isomerase) in all of our latex bead and BCG phagosomal preparations. This could reflect a contribution of the ER to formation of the phagosome, or it may reflect non-ER functions of these proteins. For example, protein-disulfide isomer-

ase A3 (Erp57), which we detected in all of our phagosome preparations, although generally considered an ER protein, has been shown also to reside in the cytosol and to form a complex with the cytosolic signaling protein STAT3 (72). Protein-disulfide isomerase, also detected in all of our phagosome preparations, has been shown to be present at high levels on the plasma membrane of lymphoid cells (72).

Specific recruitment of components of the ER to a variety of phagosomes (including those containing latex beads, zymosan, killed bacteria, and *T. gondii*) has been reported by numerous investigators based on studies of isolated phagosomes, immunoelectron microscopy, flow organellometry, and antigen processing and presentation (14, 24–27, 42, 73, 74). Most pertinent is the report by Grotzke *et al.* (28) of a specific association of ER components (including transporter associated with antigen processing (TAP) and protein-disulfide isomerase) with the *M. tuberculosis* phagosome based on flow organellometry and antigen processing and presentation studies.

The identification of numerous proteins that were found exclusively on either the BCG or latex bead phagosome, differentially expressed on one of these phagosomes relative to the other, or present at different times after phagocytosis sets the stage for further studies aimed at precisely delineating the pathway of pathogenic mycobacteria in host macrophages and the interaction of cellular organelles, macromolecular complexes, signaling proteins, trafficking proteins, enzymes, and other cellular molecules with the mycobacterial phagosome. The phagosome isolation technique described herein also allows for future studies of non-protein constituents of the mycobacterial phagosome, further elucidating the interaction of the phagosome with host cell organelles and other molecular constituents.

*Acknowledgments*—We are grateful to Matt Schibler for assistance with confocal microscopy and to Melissa Taylor for expert technical assistance.

* This work was supported, in whole or in part, by National Institutes of Health Grants HL077000 and AI065359.

S The on-line version of this article (available at http://www.mcponline.org) contains supplemental Figs. 1–4 and Tables 1–12.

¶ Present address: Bio-Rad Laboratories, 825 Alfred Noble Dr., Hercules, CA 94547.

‖ To whom correspondence should be addressed: Division of Infectious Diseases, Dept. of Medicine, UCLA School of Medicine, CHS 37-121, 10833 LeConte Ave., Los Angeles, CA 90095-1688. Tel.: 310-825-9324; Fax: 310-794-7156; E-mail: dclemens@mednet.ucla.edu.

REFERENCES

1. Xu, S., Cooper, A., Sturgill-Koszycki, S., van Heyningen, T., Chatterjee, D., Orme, I., Allen, P., and Russell, D. G. (1994) Intracellular trafficking in *Mycobacterium tuberculosis* and *Mycobacterium avium*-infected macrophages. *J. Immunol.* **153,** 2568–2578
2. Malik, Z. A., Denning, G. M., and Kusner, D. J. (2000) Inhibition of Ca(2+) signaling by *Mycobacterium tuberculosis* is associated with reduced phagosome-lysosome fusion and increased survival within human macrophages. *J. Exp. Med.* **191,** 287–302
3. Goren, M. B., D'Arcy Hart, P., Young, M. R., and Armstrong, J. A. (1976) Prevention of phagosome-lysosome fusion in cultured macrophages by sulfatides of *Mycobacterium tuberculosis. Proc. Natl. Acad. Sci. U.S.A.* **73,** 2510–2514
4. Crowle, A. J., Dahl, R., Ross, E., and May, M. H. (1991) Evidence that vesicles containing living, virulent *Mycobacterium tuberculosis* or *Mycobacterium avium* in cultured human macrophages are not acidic. *Infect. Immun.* **59,** 1823–1831
5. Armstrong, J. A., and Hart, P. D. (1971) Response of cultured macrophages to *Mycobacterium tuberculosis* with observations on fusion of lysosomes with phagosomes. *J. Exp. Med.* **134,** 713–740
6. Clemens, D. L. (1996) Characterization of the *Mycobacterium tuberculosis* phagosome. *Trends Microbiol.* **4,** 113–118
7. Clemens, D. L., and Horwitz, M. A. (1995) Characterization of the *Mycobacterium tuberculosis* phagosome and evidence that phagosomal maturation is inhibited. *J. Exp. Med.* **181,** 257–270
8. Clemens, D. L., and Horwitz, M. A. (1996) The *Mycobacterium tuberculosis* phagosome interacts with early endosomes and is accessible to exogenously administered transferrin. *J. Exp. Med.* **184,** 1349–1355
9. Clemens, D. L., Lee, B. Y., and Horwitz, M. A. (2000) *Mycobacterium tuberculosis* and *Legionella pneumophila* phagosomes exhibit arrested maturation despite acquisition of Rab7. *Infect. Immun.* **68,** 5154–5166
10. Clemens, D. L., Lee, B. Y., and Horwitz, M. A. (2000) Deviant expression of Rab5 on phagosomes containing the intracellular pathogens *Mycobacterium tuberculosis* and *Legionella pneumophila* is associated with altered phagosomal fate. *Infect. Immun.* **68,** 2671–2684
11. Via, L. E., Deretic, D., Ulmer, R. J., Hibler, N. S., Huber, L. A., and Deretic, V. (1997) Arrest of mycobacterial phagosome maturation is caused by a block in vesicle fusion between stages controlled by rab5 and rab7. *J. Biol. Chem.* **272,** 13326–13331
12. Stewart, G. R., Patel, J., Robertson, B. D., Rae, A., and Young, D. B. (2005) Mycobacterial mutants with defective control of phagosomal acidification. *PLoS Pathog.* **1,** 269–278
13. Sturgill-Koszycki, S., Schlesinger, P. H., Chakraborty, P., Haddix, P. L., Collins, H. L., Fok, A. K., Allen, R. D., Gluck, S. L., Heuser, J., and Russell, D. G. (1994) Lack of acidification in *Mycobacterium* phagosomes produced by exclusion of the vesicular proton-ATPase. *Science* **263,** 678–681
14. Garin, J., Diez, R., Kieffer, S., Dermine, J. F., Duclos, S., Gagnon, E., Sadoul, R., Rondeau, C., and Desjardins, M. (2001) The phagosome proteome: insight into phagosome functions. *J. Cell Biol.* **152,** 165–180
15. Clemens, D. L., Lee, B. Y., and Horwitz, M. A. (2002) The *Mycobacterium tuberculosis* phagosome in human macrophages is isolated from the host cell cytoplasm. *Infect. Immun.* **70,** 5800–5807
16. Lee, B. Y., Clemens, D. L., and Horwitz, M. A. (2008) The metabolic activity of *Mycobacterium tuberculosis*, assessed by use of a novel inducible GFP expression system, correlates with its capacity to inhibit phagosomal maturation and acidification in human macrophages. *Mol. Microbiol.* **68,** 1047–1060
17. Clemens, D. L., Lee, B. Y., and Horwitz, M. A. (2004) Virulent and avirulent strains of *Francisella tularensis* prevent acidification and maturation of their phagosomes and escape into the cytoplasm in human macrophages. *Infect. Immun.* **72,** 3204–3217
18. Chakraborty, P., Sturgill-Koszycki, S., and Russell, D. G. (1994) Isolation and characterization of pathogen-containing phagosomes. *Methods Cell Biol.* **45,** 261–276
19. Schilling, B., Bharath, M. M., Row, R. H., Murray, J., Cusack, M. P., Capaldi, R. A., Freed, C. R., Prasad, K. N., Andersen, J. K., and Gibson, B. W. (2005) Rapid purification and mass spectrometric characterization of mitochondrial NADH dehydrogenase (Complex I) from rodent brain and a dopaminergic neuronal cell line. *Mol. Cell. Proteomics* **4,** 84–96
20. Perkins, D. N., Pappin, D. J., Creasy, D. M., and Cottrell, J. S. (1999) Probability-based protein identification by searching sequence databases using mass spectrometry data. *Electrophoresis* **20,** 3551–3567
21. Brosch, R., Gordon, S. V., Garnier, T., Eiglmeier, K., Frigui, W., Valenti, P., Dos Santos, S., Duthoy, S., Lacroix, C., Garcia-Pelayo, C., Inwald, J. K., Golby, P., Garcia, J. N., Hewinson, R. G., Behr, M. A., Quail, M. A., Churcher, C., Barrell, B. G., Parkhill, J., and Cole, S. T. (2007) Genome plasticity of BCG and impact on vaccine efficacy. *Proc. Natl. Acad. Sci. U.S.A.* **104,** 5596–5601
22. Link, A. J., Eng, J., Schieltz, D. M., Carmack, E., Mize, G. J., Morris, D. R.,

Garvik, B. M., and Yates, J. R., 3rd (1999) Direct analysis of protein complexes using mass spectrometry. *Nat. Biotechnol.* **17,** 676–682
23. Lührmann, A., and Haas, A. (2000) A method to purify bacteria-containing phagosomes from infected macrophages. *Methods Cell Sci.* **22,** 329–341
24. Gagnon, E., Duclos, S., Rondeau, C., Chevet, E., Cameron, P. H., Steele-Mortimer, O., Paiement, J., Bergeron, J. J., and Desjardins, M. (2002) Endoplasmic reticulum-mediated phagocytosis is a mechanism of entry into macrophages. *Cell* **110,** 119–131
25. Giodini, A., Rahner, C., and Cresswell, P. (2009) Receptor-mediated phagocytosis elicits cross-presentation in nonprofessional antigen-presenting cells. *Proc. Natl. Acad. Sci. U.S.A.* **106,** 3324–3329
26. Ackerman, A. L., Kyritsis, C., Tampé, R., and Cresswell, P. (2003) Early phagosomes in dendritic cells form a cellular compartment sufficient for cross presentation of exogenous antigens. *Proc. Natl. Acad. Sci. U.S.A.* **100,** 12889–12894
27. Goldszmid, R. S., Coppens, I., Lev, A., Caspar, P., Mellman, I., and Sher, A. (2009) Host ER-parasitophorous vacuole interaction provides a route of entry for antigen cross-presentation in *Toxoplasma gondii*-infected dendritic cells. *J. Exp. Med.* **206,** 399–410
28. Grotzke, J. E., Harriff, M. J., Siler, A. C., Nolt, D., Delepine, J., Lewinsohn, D. A., and Lewinsohn, D. M. (2009) The *Mycobacterium tuberculosis* phagosome is a HLA-I processing competent organelle. *PLoS Pathog.* **5,** e1000374
29. Touret, N., Paroutis, P., Terebiznik, M., Harrison, R. E., Trombetta, S., Pypaert, M., Chow, A., Jiang, A., Shaw, J., Yip, C., Moore, H. P., van der Wel, N., Houben, D., Peters, P. J., de Chastellier, C., Mellman, I., and Grinstein, S. (2005) Quantitative and dynamic assessment of the contribution of the ER to phagosome formation. *Cell* **123,** 157–170
30. Royle, S. J. (2006) The cellular functions of clathrin. *Cell. Mol. Life Sci.* **63,** 1823–1832
31. Katoh, K., Shibata, H., Suzuki, H., Nara, A., Ishidoh, K., Kominami, E., Yoshimori, T., and Maki, M. (2003) The ALG-2-interacting protein Alix associates with CHMP4b, a human homologue of yeast Snf7 that is involved in multivesicular body sorting. *J. Biol. Chem.* **278,** 39104–39113
32. Katoh, K., Shibata, H., Hatta, K., and Maki, M. (2004) CHMP4b is a major binding partner of the ALG-2-interacting protein Alix among the three CHMP4 isoforms. *Arch. Biochem. Biophys.* **421,** 159–165
33. Février, B., and Raposo, G. (2004) Exosomes: endosomal-derived vesicles shipping extracellular messages. *Curr. Opin. Cell Biol.* **16,** 415–421
34. Wubbolts, R., Leckie, R. S., Veenhuizen, P. T., Schwarzmann, G., Möbius, W., Hoernschemeyer, J., Slot, J. W., Geuze, H. J., and Stoorvogel, W. (2003) Proteomic and biochemical analyses of human B cell-derived exosomes. Potential implications for their function and multivesicular body formation. *J. Biol. Chem.* **278,** 10963–10972
35. de Gassart, A., Geminard, C., Fevrier, B., Raposo, G., and Vidal, M. (2003) Lipid raft-associated protein sorting in exosomes. *Blood* **102,** 4336–4344
36. Shakibaei, M., Zimmermann, B., and Scheller, M. (1993) Endocytosis of integrin alpha 5 beta 1 (fibronectin receptor) of mouse peritoneal macrophages in vitro: an immunoelectron microscopic study. *J. Struct. Biol.* **111,** 180–189
37. Dermine, J. F., Duclos, S., Garin, J., St-Louis, F., Rea, S., Parton, R. G., and Desjardins, M. (2001) Flotillin-1-enriched lipid raft domains accumulate on maturing phagosomes. *J. Biol. Chem.* **276,** 18507–18512
38. Snyers, L., Umlauf, E., and Prohaska, R. (1999) Association of stomatin with lipid-protein complexes in the plasma membrane and the endocytic compartment. *Eur. J. Cell Biol.* **78,** 802–812
39. Browman, D. T., Resek, M. E., Zajchowski, L. D., and Robbins, S. M. (2006) Erlin-1 and erlin-2 are novel members of the prohibitin family of proteins that define lipid-raft-like domains of the ER. *J. Cell Sci.* **119,** 3149–3160
40. Hofmann, I., and Munro, S. (2006) An N-terminally acetylated Arf-like GTPase is localised to lysosomes and affects their motility. *J. Cell Sci.* **119,** 1494–1503
41. Maekawa, S., Iino, S., and Miyata, S. (2003) Molecular characterization of the detergent-insoluble cholesterol-rich membrane microdomain (raft) of the central nervous system. *Biochim. Biophys. Acta* **1610,** 261–270
42. Stuart, L. M., Boulais, J., Charriere, G. M., Hennessy, E. J., Brunet, S., Jutras, I., Goyette, G., Rondeau, C., Letarte, S., Huang, H., Ye, P., Morales, F., Kocks, C., Bader, J. S., Desjardins, M., and Ezekowitz, R. A. (2007) A systems biology analysis of the Drosophila phagosome. *Nature* **445,** 95–101
43. Oldham, W. M., and Hamm, H. E. (2008) Heterotrimeric G protein activation by G-protein-coupled receptors. *Nat. Rev. Mol. Cell Biol.* **9,** 60–71
44. Brown, M. D., and Sacks, D. B. (2006) IQGAP1 in cellular signaling: bridging the GAP. *Trends Cell Biol.* **16,** 242–249
45. Mrowiec, T., and Schwappach, B. (2006) 14-3-3 proteins in membrane protein transport. *Biol. Chem.* **387,** 1227–1236
46. Hubberstey, A. V., and Mottillo, E. P. (2002) Cyclase-associated proteins: CAPacity for linking signal transduction and actin polymerization. *FASEB J.* **16,** 487–499
47. Damiani, M. T., Pavarotti, M., Leiva, N., Lindsay, A. J., McCaffrey, M. W., and Colombo, M. I. (2004) Rab coupling protein associates with phagosomes and regulates recycling from the phagosomal compartment. *Traffic* **5,** 785–797
48. Sannerud, R., Marie, M., Nizak, C., Dale, H. A., Pernet-Gallay, K., Perez, F., Goud, B., and Saraste, J. (2006) Rab1 defines a novel pathway connecting the pre-Golgi intermediate compartment with the cell periphery. *Mol. Biol. Cell* **17,** 1514–1526
49. Miserey-Lenkei, S., Waharte, F., Boulet, A., Cuif, M. H., Tenza, D., El Marjou, A., Raposo, G., Salamero, J., Héliot, L., Goud, B., and Monier, S. (2007) Rab6-interacting protein 1 links Rab6 and Rab11 function. *Traffic* **8,** 1385–1403
50. Simpson, J. C., Griffiths, G., Wessling-Resnick, M., Fransen, J. A., Bennett, H., and Jones, A. T. (2004) A role for the small GTPase Rab21 in the early endocytic pathway. *J. Cell Sci.* **117,** 6297–6311
51. Pellinen, T., Arjonen, A., Vuoriluoto, K., Kallio, K., Fransen, J. A., and Ivaska, J. (2006) Small GTPase Rab21 regulates cell adhesion and controls endosomal traffic of beta1-integrins. *J. Cell Biol.* **173,** 767–780
52. Kyei, G. B., Vergne, I., Chua, J., Roberts, E., Harris, J., Junutula, J. R., and Deretic, V. (2006) Rab14 is critical for maintenance of *Mycobacterium tuberculosis* phagosome maturation arrest. *EMBO J.* **25,** 5250–5259
53. Rossé, C., Hatzoglou, A., Parrini, M. C., White, M. A., Chavrier, P., and Camonis, J. (2006) RalB mobilizes the exocyst to drive cell migration. *Mol. Cell. Biol.* **26,** 727–734
54. Li, G., Han, L., Chou, T. C., Fujita, Y., Arunachalam, L., Xu, A., Wong, A., Chiew, S. K., Wan, Q., Wang, L., and Sugita, S. (2007) RalA and RalB function as the critical GTP sensors for GTP-dependent exocytosis. *J. Neurosci.* **27,** 190–202
55. Oxford, G., Owens, C. R., Titus, B. J., Foreman, T. L., Herlevsen, M. C., Smith, S. C., and Theodorescu, D. (2005) RalA and RalB: antagonistic relatives in cancer cell migration. *Cancer Res.* **65,** 7111–7120
56. Chien, Y., Kim, S., Bumeister, R., Loo, Y. M., Kwon, S. W., Johnson, C. L., Balakireva, M. G., Romeo, Y., Kopelovich, L., Gale, M., Jr., Yeaman, C., Camonis, J. H., Zhao, Y., and White, M. A. (2006) RalB GTPase-mediated activation of the IkappaB family kinase TBK1 couples innate immune signaling to tumor cell survival. *Cell* **127,** 157–170
57. Pizon, V., Desjardins, M., Bucci, C., Parton, R. G., and Zerial, M. (1994) Association of Rap1a and Rap1b proteins with late endocytic/phagocytic compartments and Rap2a with the Golgi complex. *J. Cell Sci.* **107,** 1661–1670
58. Théry, C., Boussac, M., Véron, P., Ricciardi-Castagnoli, P., Raposo, G., Garin, J., and Amigorena, S. (2001) Proteomic analysis of dendritic cell-derived exosomes: a secreted subcellular compartment distinct from apoptotic vesicles. *J. Immunol.* **166,** 7309–7318
59. Li, Y., Yan, J., De, P., Chang, H. C., Yamauchi, A., Christopherson, K. W., 2nd, Paranavitana, N. C., Peng, X., Kim, C., Munugalavadla, V., Kapur, R., Chen, H., Shou, W., Stone, J. C., Kaplan, M. H., Dinauer, M. C., Durden, D. L., and Quilliam, L. A. (2007) Rap1a null mice have altered myeloid cell functions suggesting distinct roles for the closely related Rap1a and 1b proteins. *J. Immunol.* **179,** 8322–8331
60. Bernardi, B., Guidetti, G. F., Campus, F., Crittenden, J. R., Graybiel, A. M., Balduini, C., and Torti, M. (2006) The small GTPase Rap1b regulates the cross talk between platelet integrin alpha2beta1 and integrin alphaIIb-beta3. *Blood* **107,** 2728–2735
61. Fratti, R. A., Chua, J., and Deretic, V. (2003) Induction of p38 mitogen-activated protein kinase reduces early endosome autoantigen 1 (EEA1) recruitment to phagosomal membranes. *J. Biol. Chem.* **278,** 46961–46967
62. Cavalli, V., Vilbois, F., Corti, M., Marcote, M. J., Tamura, K., Karin, M., Arkinstall, S., and Gruenberg, J. (2001) The stress-induced MAP kinase p38 regulates endocytic trafficking via the GDI:Rab5 complex. *Mol. Cell*

**7,** 421–432
63. Kollmann, K., Mutenda, K. E., Balleininger, M., Eckermann, E., von Figura, K., Schmidt, B., and Lübke, T. (2005) Identification of novel lysosomal matrix proteins by proteome analysis. *Proteomics* **5,** 3966–3978
64. Pilipenko, V. V., Reece, A., Choo, D. I., and Greinwald, J. H., Jr. (2004) Genomic organization and expression analysis of the murine Fam3c gene. *Gene* **335,** 159–168
65. Reynolds, J. L., Mahajan, S. D., Sykes, D., and Nair, M. P. (2006) Heroin-Induces Differential Protein Expression by Normal Human Astrocytes (NHA). *Am. J. Infect. Dis.* **2,** 49–57
66. Li, D. Q., Wang, L., Fei, F., Hou, Y. F., Luo, J. M., Zeng, R., Wu, J., Lu, J. S., Di, G. H., Ou, Z. L., Xia, Q. C., Shen, Z. Z., and Shao, Z. M. (2006) Identification of breast cancer metastasis-associated proteins in an isogenic tumor metastasis model using two-dimensional gel electrophoresis and liquid chromatography-ion trap-mass spectrometry. *Proteomics* **6,** 3352–3368
67. Brasaemle, D. L., Dolios, G., Shapiro, L., and Wang, R. (2004) Proteomic analysis of proteins associated with lipid droplets of basal and lipolytically stimulated 3T3-L1 adipocytes. *J. Biol. Chem.* **279,** 46835–46842
68. Hayess, K., Kraft, R., Sachsinger, J., Janke, J., Beckmann, G., Rohde, K., Jandrig, B., and Benndorf, R. (1998) Mammalian protein homologous to VAT-1 of Torpedo californica: isolation from Ehrlich ascites tumor cells, biochemical characterization, and organization of its gene. *J. Cell. Biochem.* **69,** 304–315
69. Persson, B., Zigler, J. S., Jr., and Jörnvall, H. (1994) A super-family of medium-chain dehydrogenases/reductases (MDR). Sub-lines including zeta-crystallin, alcohol and polyol dehydrogenases, quinone oxidoreductase enoyl reductases, VAT-1 and other proteins. *Eur. J. Biochem.* **226,** 15–22
70. Koch, J., Foekens, J., Timmermans, M., Fink, W., Wirzbach, A., Kramer, M. D., and Schaefer, B. M. (2003) Human VAT-1: a calcium-regulated activation marker of human epithelial cells. *Arch. Dermatol. Res.* **295,** 203–210
71. Li, N., Mak, A., Richards, D. P., Naber, C., Keller, B. O., Li, L., and Shaw, A. R. (2003) Monocyte lipid rafts contain proteins implicated in vesicular trafficking and phagosome formation. *Proteomics* **3,** 536–548
72. Turano, C., Coppari, S., Altieri, F., and Ferraro, A. (2002) Proteins of the PDI family: unpredicted non-ER locations and functions. *J. Cell. Physiol.* **193,** 154–163
73. Houde, M., Bertholet, S., Gagnon, E., Brunet, S., Goyette, G., Laplante, A., Princiotta, M. F., Thibault, P., Sacks, D., and Desjardins, M. (2003) Phagosomes are competent organelles for antigen cross-presentation. *Nature* **425,** 402–406
74. Desjardins, M. (2003) ER-mediated phagocytosis: a new membrane for new functions. *Nat. Rev. Immunol.* **3,** 280–291
75. Brudzynski, K., Martinez, V., and Gupta, R. S. (1992) Secretory granule autoantigen in insulin-dependent diabetes mellitus is related to 62 kDa heat-shock protein (hsp60). *J. Autoimmun.* **5,** 453–463
76. Cechetto, J. D., Soltys, B. J., and Gupta, R. S. (2000) Localization of mitochondrial 60-kD heat shock chaperonin protein (Hsp60) in pituitary growth hormone secretory granules and pancreatic zymogen granules. *J. Histochem. Cytochem.* **48,** 45–56
77. Brudzynski, K., Martinez, V., and Gupta, R. S. (1992) Immunocytochemical localization of heat-shock protein 60-related protein in beta-cell secretory granules and its altered distribution in non-obese diabetic mice. *Diabetologia* **35,** 316–324
78. Schindler, R., Weichselsdorfer, E., Wagner, O., and Bereiter-Hahn, J. (2001) Aldolase-localization in cultured cells: cell-type and substrate-specific regulation of cytoskeletal associations. *Biochem. Cell Biol.* **79,** 719–728
79. Liu, L., Yang, C., Yuan, J., Chen, X., Xu, J., Wei, Y., Yang, J., Lin, G., and Yu, L. (2005) RPK118, a PX domain-containing protein, interacts with peroxiredoxin-3 through pseudo-kinase domains. *Mol. Cells* **19,** 39–45
80. Sirover, M. A. (1999) New insights into an old protein: the functional diversity of mammalian glyceraldehyde-3-phosphate dehydrogenase. *Biochim. Biophys. Acta* **1432,** 159–184
81. Buettner, R., Papoutsoglou, G., Scemes, E., Spray, D. C., and Dermietzel, R. (2000) Evidence for secretory pathway localization of a voltage-dependent anion channel isoform. *Proc. Natl. Acad. Sci. U.S.A.* **97,** 3201–3206
82. Sadacharan, S. K., Cavanagh, A. C., and Gupta, R. S. (2001) Immunoelectron microscopy provides evidence for the presence of mitochondrial heat shock 10-kDa protein (chaperonin 10) in red blood cells and a variety of secretory granules. *Histochem. Cell Biol.* **116,** 507–517
83. Liu, H., Sadygov, R. G., and Yates, J. R., 3rd (2004) A model for random sampling and estimation of relative protein abundance in shotgun proteomics. *Anal. Chem.* **76,** 4193–4201